



# Low-Dose Rectal Inoculation of Rhesus Macaques by SIVsmE660 or SIVmac251 Recapitulates Human Mucosal Infection by HIV-1

## Citation

Keele, Brandon F., Hui Li, Gerald H. Learn, Peter Hraber, Elena E. Giorgi, Truman Grayson, Chuanxi Sun, et al. 2009. Low-dose rectal inoculation of rhesus macaques by SIVsmE660 or SIVmac251 recapitulates human mucosal infection by HIV-1. *Journal of Experimental Medicine* 206(5): 1117-1134.

## Published Version

doi: 10.1084/jem.20082831

## Permanent link

<http://nrs.harvard.edu/urn-3:HUL.InstRepos:4621131>

## Terms of Use

This article was downloaded from Harvard University's DASH repository, and is made available under the terms and conditions applicable to Other Posted Material, as set forth at <http://nrs.harvard.edu/urn-3:HUL.InstRepos:dash.current.terms-of-use#LAA>

## Share Your Story

The Harvard community has made this article openly available.  
Please share how this access benefits you. [Submit a story](#).

[Accessibility](#)

# Low-dose rectal inoculation of rhesus macaques by SIVsmE660 or SIVmac251 recapitulates human mucosal infection by HIV-1

Brandon F. Keele,<sup>1</sup> Hui Li,<sup>1</sup> Gerald H. Learn,<sup>1</sup> Peter Hraber,<sup>2</sup> Elena E. Giorgi,<sup>2,3</sup> Truman Grayson,<sup>1</sup> Chuanxi Sun,<sup>1</sup> Yalu Chen,<sup>1</sup> Wendy W. Yeh,<sup>4</sup> Norman L. Letvin,<sup>4,5</sup> John R. Mascola,<sup>5</sup> Gary J. Nabel,<sup>5</sup> Barton F. Haynes,<sup>6</sup> Tanmoy Bhattacharya,<sup>2,7</sup> Alan S. Perelson,<sup>2</sup> Bette T. Korber,<sup>2,7</sup> Beatrice H. Hahn,<sup>1</sup> and George M. Shaw<sup>1</sup>

<sup>1</sup>University of Alabama at Birmingham, Birmingham, AL 35223

<sup>2</sup>Los Alamos National Laboratory, Los Alamos, NM 87545

<sup>3</sup>University of Massachusetts, Amherst, MA 01002

<sup>4</sup>Division of Viral Pathogenesis, Department of Medicine, Beth Israel Deaconess Medical Center, Harvard Medical School, Boston, MA 02115

<sup>5</sup>Vaccine Research Center, National Institute of Allergy and Infectious Disease, National Institutes of Health, Bethesda, MD 20892

<sup>6</sup>Duke University Medical Center, Durham, NC 27710

<sup>7</sup>Santa Fe Institute, Santa Fe, NM 87501

We recently developed a novel strategy to identify transmitted HIV-1 genomes in acutely infected humans using single-genome amplification and a model of random virus evolution. Here, we used this approach to determine the molecular features of simian immunodeficiency virus (SIV) transmission in 18 experimentally infected Indian rhesus macaques. Animals were inoculated intrarectally (i.r.) or intravenously (i.v.) with stocks of SIVmac251 or SIVsmE660 that exhibited sequence diversity typical of early-chronic HIV-1 infection. 987 full-length SIV *env* sequences (median of 48 per animal) were determined from plasma virion RNA 1–5 wk after infection. i.r. inoculation was followed by productive infection by one or a few viruses (median 1; range 1–5) that diversified randomly with near starlike phylogeny and a Poisson distribution of mutations. Consensus viral sequences from ramp-up and peak viremia were identical to viruses found in the inocula or differed from them by only one or a few nucleotides, providing direct evidence that early plasma viral sequences coalesce to transmitted/founder viruses. i.v. infection was >2,000-fold more efficient than i.r. infection, and viruses transmitted by either route represented the full genetic spectra of the inocula. These findings identify key similarities in mucosal transmission and early diversification between SIV and HIV-1, and thus validate the SIV-macaque mucosal infection model for HIV-1 vaccine and microbicide research.

## CORRESPONDENCE

George M. Shaw:  
gshaw@uab.edu

Abbreviations used: CI, confidence interval; HD, Hamming distance; i.r., intrarectally; MRCA, most recent common ancestor; NJ, neighbor-joining; SGA, single-genome amplification; SIV, simian immunodeficiency virus; vRNA, viral RNA.

An effective HIV-1 vaccine, microbicide, or other pre- or post-exposure prophylactic must interdict virus at or near the moment of mucosal transmission or in the early period preceding the establishment of viral latency and disseminated infection (1–4). In humans, it has been difficult to study these earliest viral host events in vivo (2, 5–13), and in tissue explant cultures or in Indian rhesus macaques the HIV-1 or simian immunodeficiency virus (SIV) inocula have typically been high to

achieve uniform infection of controls or to visualize infection events in situ (14–20), thus prompting concerns about the physiological relevance of the model systems (21–24). Further complicating the analysis of early infection events in vivo is the viral “eclipse”

© 2009 Keele et al. This article is distributed under the terms of an Attribution–Noncommercial–Share Alike–No Mirror Sites license for the first six months after the publication date (see <http://www.jem.org/misc/terms.shtml>). After six months it is available under a Creative Commons License (Attribution–Noncommercial–Share Alike 3.0 Unported license, as described at <http://creativecommons.org/licenses/by-nc-sa/3.0/>).

period during which virus replicates in mucosal and local lymphoreticular tissues but is not yet detectable in the circulating plasma (25). In SIV-infected macaques, the eclipse period is generally  $\sim 4\text{--}7$  d in duration, and in HIV-1-infected humans, it is  $\sim 7\text{--}21$  d (5, 18, 25–27).

Previously, we observed that in the early stages of HIV-1 infection preceding antibody seroconversion (eclipse phase and Fiebig stages I and II [25]), virus diversification follows a pattern of random evolution with an almost starlike phylogeny and a Poisson distribution of nucleotide substitutions (5). We thus hypothesized that the genetic identity of transmitted or early founder viruses could be inferred unambiguously by phylogenetic analysis of discrete low-diversity viral lineages that emanate from them. This hypothesis was supported by an analysis of 3,449 full-length *env* genes from 102 human subjects with acute HIV-1 subtype B infection, where we found that (a) acute viral sequences sampled before the development of measurable adaptive immune responses conformed to a pattern of random virus evolution; (b) viral sequence diversity resulted in model estimates of time to a most recent common ancestor (MRCA) that was consistent with clinical histories and Fiebig stage classifications; and (c) in most subjects (78 of 102) there was evidence of productive infection by only a single virus, whereas in 24 other subjects infection resulted from transmission of at least 2 to 5 viruses, each recognizable as a discrete virus lineage (5). These findings have since been corroborated in seven additional patient cohorts infected by HIV-1 subtypes A, B, C, or D (28–35). A key innovation common to these studies was the use of single-genome amplification (SGA) of plasma viral RNA, followed by direct amplicon sequencing to characterize the virus quasispecies (5, 35–39). This method provides proportional representation of plasma viral RNA (vRNA) and precludes *Taq* polymerase-induced template switching (recombination), *Taq* polymerase-associated nucleotide substitutions in finished sequences, template resampling, and cloning bias (5, 35, 37, 38, 40).

In this study, we sought to directly test our strategy for identifying transmitted/founder viruses in the Indian rhesus macaque SIV infection model where we could define essential experimental parameters, including the route of SIV infection, genetic composition of the inoculum, and the duration between virus inoculation and sampling of plasma vRNA. The primary study objectives were two-fold: first, to determine if, as our hypothesis and model predict, plasma SIV sequences sampled at or near peak viremia coalesce to sequences of viruses responsible for transmission and productive clinical infection weeks earlier; and second, to determine how closely a low-dose SIV rectal transmission model in Indian rhesus macaques recapitulates features of human infection by HIV-1, including the extent of the mucosal barrier to virus transmission, the number of transmitted/founder viruses leading to productive infection, and the molecular patterns of early virus diversification.

## RESULTS

### Inoculation regimen and infection kinetics

18 animals received weekly atraumatic i.r. inoculations of cell-free SIV as part of a previous study of adaptive immune responses after mucosal virus exposure (41). The virus inocula were uncloned SIVmac251 or SIVsmE660 strains comprised of virus “swarms” with *env* diversity comparable to what is observed in humans 1–2 yr after infection by HIV-1 (42). 9 animals, divided into groups of 3, received log dilutions of  $6 \times 10^7$ ,  $6 \times 10^6$ , or  $6 \times 10^5$  vRNA copies of SIVsmE660 (Fig. 1, left). Nine other animals, divided into groups of three, received identical dilutions of SIVmac251 (Fig. 1, right). Virus was administered weekly for 6 wk, followed by a 3-wk observation period and a 2-mo rest period to ensure that none of the animals experienced delayed seroconversion. Animals were phlebotomized weekly during the inoculation–observation period. Animals that did not become productively infected after the first inoculation–observation–rest cycle underwent a second 6-wk course of i.r. inoculations at the same virus dose level, followed by a 3-wk observation period and a 2-mo rest period. Animals that still did not become infected underwent a third 6-wk course of i.r. inoculations at the maximum virus dose level ( $6 \times 10^7$  vRNA copies), followed by observation and rest periods. One animal, AV66, received SIVsmE660 for the initial two i.r. inoculation cycles and was then crossed over to receive SIVmac251 for the third i.r. inoculation cycle (Fig. 1, bottom left). 5 animals that did not become infected after the 18 i.r. inoculations were given a single i.v. inoculation of  $2 \times 10^5$  vRNA copies. All animals became infected.

The kinetics of virus infection and replication, and the time points of plasma virus sampling for *env* sequence analysis, are illustrated (Fig. 1). There was no significant difference in the overall infection rate between macaques inoculated i.r. with SIVsmE660 (6 of 8 animals) versus SIVmac251 (7 of 10 animals). Because of this similarity, and the relatively small number of animals in the study ( $n = 18$ ), the 6 animals in each virus dose group were combined for purposes of statistical analysis. We found a statistically significant virus dose–infection trend to i.r. infection, with 6 of 6 animals receiving the highest dose of SIV becoming infected in the first 8 wk inoculation–observation regimen, 4 of 6 animals receiving the intermediate dose becoming infected in the same period, and 1 of 6 animals receiving the lowest dose becoming infected in the same period ( $P = 0.005$  by  $3 \times 2$  Fisher’s exact test). Two animals, AV66 and AH4X, did not become infected after 12 weekly i.r. inoculations at the lowest dose of virus ( $6 \times 10^5$  vRNA copies), but did become infected after 1–4 i.r. inoculations at the highest virus dose ( $6 \times 10^7$  vRNA copies). 5 animals, CP37, CR54, AV74, CG71, and CG5G, did not become infected even after 18 weekly i.r. inoculations, but each became infected after a single i.v. inoculation. For both SIVsmE660- and SIVmac251-infected animals, the kinetics of plasma viral load increase were quite similar, reaching peak viremia within 1 wk of the last negative sample in three animals and within 2 wk in 15 others. Peak viral

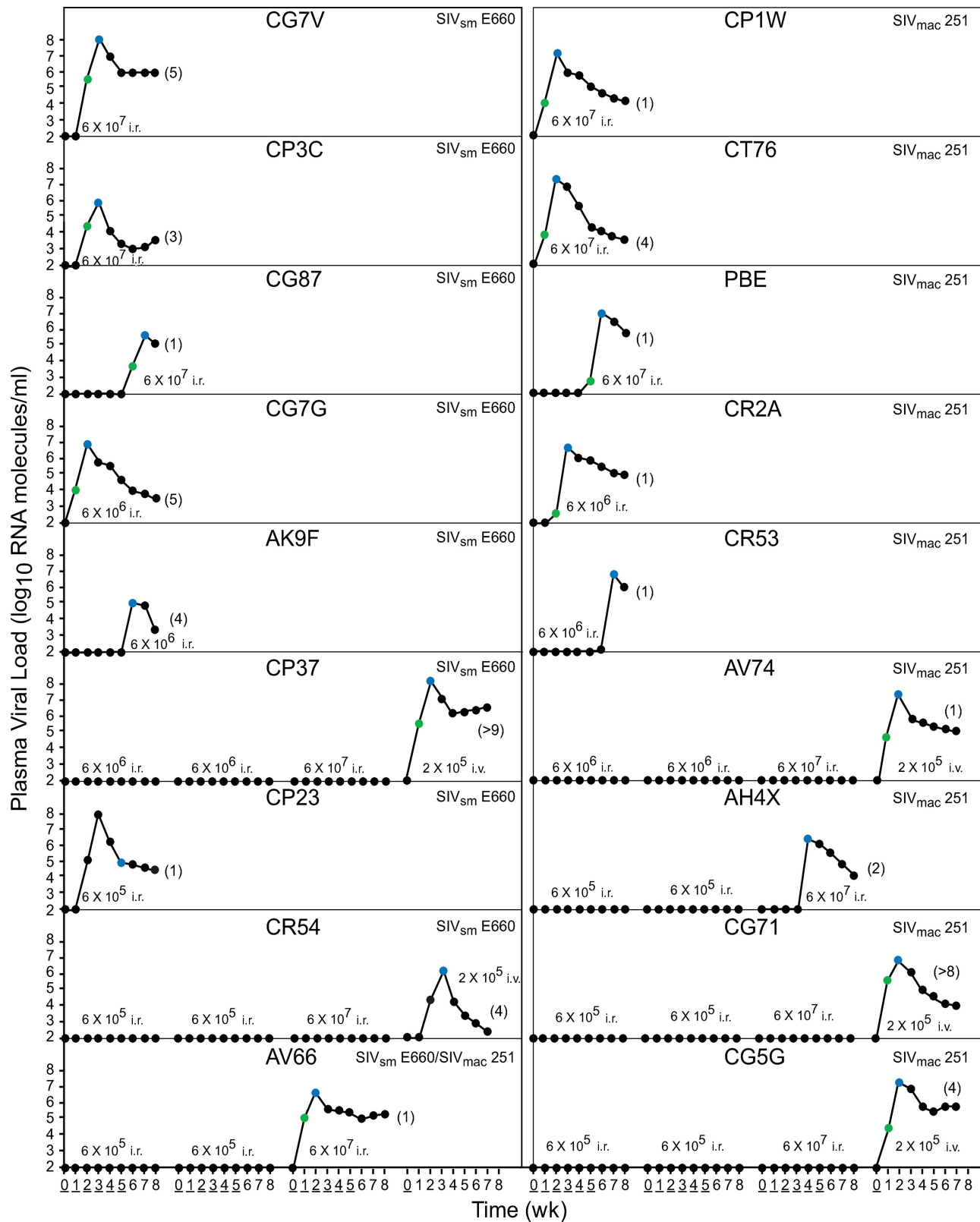


**Figure 1. Viral kinetics after i.r. or i.v. infection.** Groups of three animals received i.r. inoculations of SIVsmE660 or SIVmac251 in dosages indicated at weeks 0, 1, 2, 3, 4, and 5 (underlined) or by the i.v. route at week 0 (only) of the fourth cycle. Plasma was sampled at ramp-up (green symbols) or at peak (blue symbols) viremia for *env* sequence analysis. Numbers of transmitted/founder viruses found to be responsible for productive infection are indicated in parenthesis. Plasma viral load determinations were previously reported (41).



loads ranged from  $1.4 \times 10^5$  to  $9.4 \times 10^7$  (median  $8 \times 10^6$ ) and were not related to the infecting virus strain or route of infection. A correlation between peak viral load and numbers of transmitted viruses was observed for SIVsmE660-infected (Spearman correlation coefficient 0.71;  $P = 0.05$ ) and SIVmac251-infected (Spearman correlation coefficient 0.91;  $P = 0.005$ ) macaques.

### Virus diversity in SIV inoculum stocks

The extent of virus sequence diversity in the inoculum stocks of SIVsmE660 and SIVmac251 was determined by SGA-direct sequencing of full-length vRNA *env* genes, followed by pairwise sequence comparisons, neighbor-joining (NJ) phylogenetic tree construction, and *Highlighter* analysis (Fig. S1). *Highlighter* is a sequence analytical tool ([www.HIV.lanl.gov](http://www.HIV.lanl.gov)) that displays the location and identity of nucleotide substitutions in a visually informative manner and allows tracing of common ancestry between sequences based on individual nucleotide polymorphisms. Maximum diversity among 42 SIVsmE660 *env* sequences was 1.8%, and among 61 SIVmac251 sequences, diversity was 0.8%. NJ trees of both sequence sets revealed structure in the phylogenetic relationships among sequences typical of primary virus isolates. *Highlighter* plots reflected this structured diversity.

### Virus diversity in SIV-infected macaques

A total of 987 full-length SIV *env* genes of plasma virions from 18 animals (median of 48 per animal; range 23–137) were amplified and sequenced. 26 sequences (distributed among 12 animals) showed evidence of overt APOBEC G-to-A hypermutation (e.g., sequences RU.I3, RU.4B7, PK.I6, PK.4A29 and PK.I10 in Fig. 2). These sequences were retained in phylogenetic tree constructions but were excluded from diversity measurements and model calculations. Among the remaining 961 sequences, maximum *env* diversity in animals infected i.r. ranged from 0.07 to 1.43% (median = 0.33%). Maximum *env* diversity in animals infected intravenously ranged from 0.18 to 1.54% (median = 0.81%), which is not different from viral diversity in i.r.-infected animals ( $P = 0.11$  by Wilcoxon rank sum test). i.r.-infected animals had *env* sequence diversities that fell into two distinctive groups, which we showed subsequently to reflect productive infection by one virus (maximum *env* diversity of 0.07–0.15%, median = 0.15%) or more than one virus (maximum *env* diversity of 0.59–1.43%, median = 0.95%;  $P = 0.0003$  by Student's *t* test of a generalized linear model of maximum *env* diversity).

Sequence diversity in animal CP1W, which was infected by the i.r. route, is illustrated by a NJ tree comprised of 137 *env* sequences from ramp-up (green ovals) and peak (blue ovals) viremia along with 61 sequences from the SIVmac251 inoculum (black ovals; Fig. 2 A). 102 of 137 CP1W *env* sequences were identical to themselves and to 4 sequences (K11, K9, G2, and TB2L) in the inoculum. 22 other CP1W *env* sequences differed from this consensus CP1W *env* sequence by 1 nt, and 8 CP1W *env* sequences differed from the consensus by 2 nt. Most of these 30 sequences differed from the consensus by unique mutations, which is consistent with

an almost starlike phylogeny (Fig. 2, A and B). Five other CP1W *env* sequences (RU.I3, RU.4B7, PK.I6, PK.4A29, and PK.I10) differed from the consensus by 3–7 nt, but these were notable for APOBEC-related G-to-A hypermutation (Fig. 2, A and B). Ramp-up sequences sampled 1 wk after infection, and peak viremia samples obtained 2 wk after infection, each coalesced to the same consensus sequence, which was identical to sequences in the inoculum. Thus, a single virus established productive clinical infection in CP1W, and it could be traced back from peak viremia through the eclipse phase of infection to the moment of transmission and into the inoculum.

Single, low-diversity viral lineages with starlike phylogeny and Poisson distributed substitutions were also found in i.r.-infected animals PBE (Fig. 3 A), CG87 (Fig. 4 A), AV66, CR2A, and CR53 (Table I). In each animal, sequences from ramp-up and peak viremia coalesced to single consensus sequences representing transmitted/founder viruses. In two of these animals (PBE and CR2A), the transmitted/founder viruses differed from sequences identified in the inoculum by only 2 nt. In another i.r.-infected animal (CP23), ramp-up and peak viremia samples were not available for analysis, so we instead analyzed samples taken 2 wk after peak viremia, corresponding to 4–5 wk after infection (Fig. 1). The phylogenetic tree of CP23 sequences was distinctly different from the phylogenies of sequences from all other animals (Fig. S2). The *Highlighter* plot revealed an extraordinary concentration of unique and shared mutations confined to a short stretch of 19 nt in the gp41 coding region of *env* overlapping the *nef* gene (Fig. S2). Here, 32 out of 37 sequences in the *env* reading frame, and 34 out of 37 sequences in the *nef* reading frame, contained amino acid substitutions compared with the transmitted/founder sequence and the consensus of sequences present in the SIVsmE660 inoculum. The clustered mutations in the Env reading frame were contiguous with a 9-mer Env peptide (FHEAVQAVW) corresponding to a known Mamu-B\*17-restricted CTL epitope (43). Animal CP23 was Mamu-B\*17 positive. These findings thus indicated that monkey CP23 was infected by a single virus, but that this virus evolved extremely rapidly, most likely as a consequence of CTL selection pressure, such that by 4–5 wk after infection, >85% of viral sequences were escape variants. Similar patterns and kinetics of rapid CTL escape have been reported for SIV and HIV-1 (5, 30, 35, 44, 45).

Six other animals (CG7V, CP3C, CG7G, AK9F, CT76, and AH4X) were infected by i.r. virus inoculations but showed substantially greater maximum pairwise diversity among their sequences (0.59–1.43%) than did the animals that were productively infected by only a single virus (0.07–0.15%, excluding CP23). NJ trees and *Highlighter* plots of sequences from these six animals revealed two or more discrete low-diversity *env* lineages, each representing a distinct transmitted/founder virus (Figs. 5, 6, and S4). Overall, there was a trend observed between the virus inoculum dose that each animal received and the number of transmitted viral

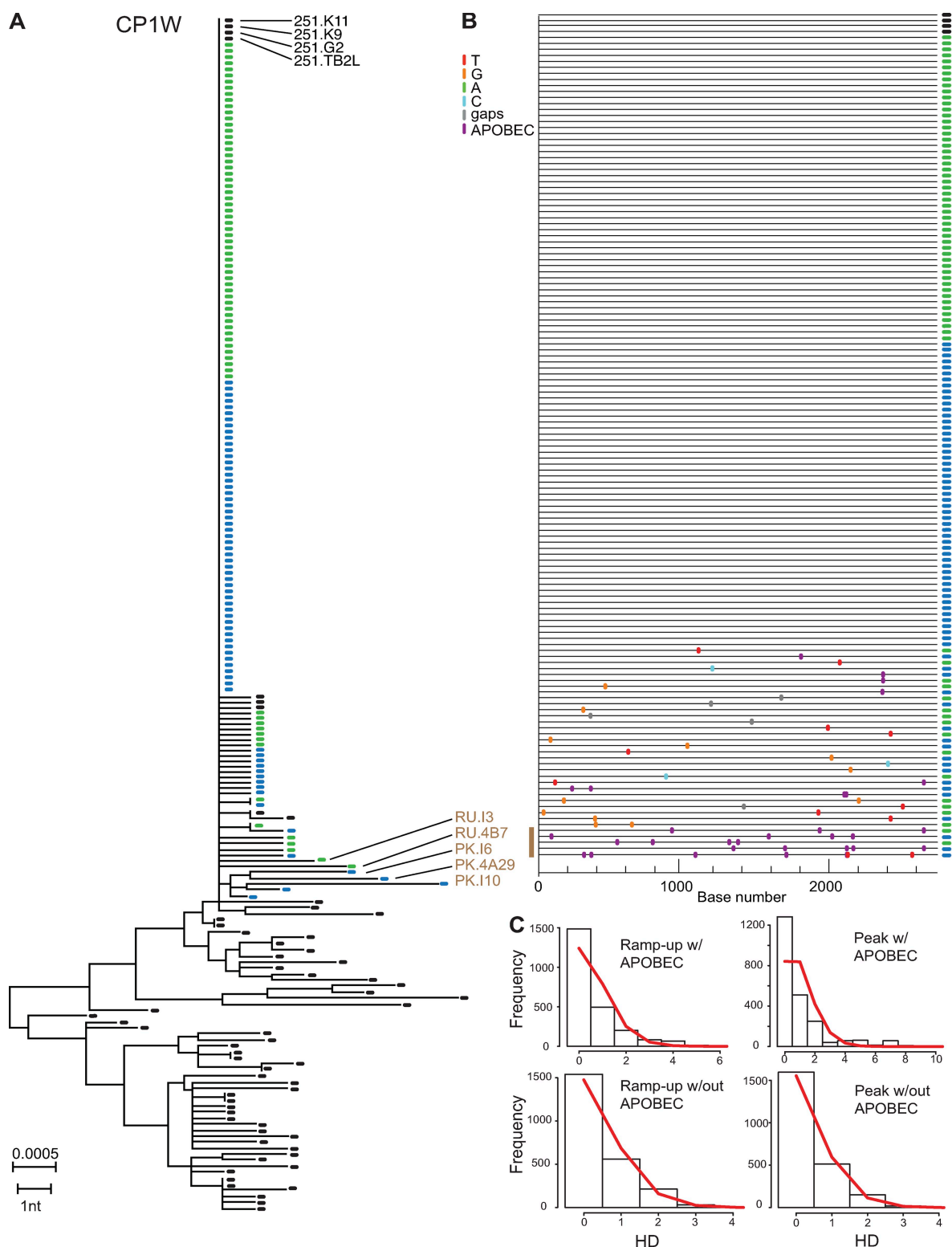


**Figure 2. Viral sequence analysis after intrarectal SIVmac251 infection of animal CP1W.** (A) NJ tree of sequences from ramp-up (green symbols) or peak (blue symbols) viremia or from the inoculum (black symbols). (B) *Highlighter* alignment of all CP1W sequences compared with four identical sequences from the inoculum and to the transmitted/founder virus. Nucleotide polymorphisms are indicated by a colored tic mark (thymine in red, guanine in orange, adenine in green, and cytosine in blue). APOBEC-mediated G-to-A mutations are indicated by purple tics, and deletions are indicated by gray tics. (C) Poisson model of early viral diversity. Brown labels indicate sequences with three or more APOBEC-mediated G-to-A mutations compared with consensus.

variants leading to productive clinical infection: among the 12 animals receiving the two highest doses of virus in the initial inoculation–observation cycle, a minimum of 26 viruses were transmitted to 10 animals. Among the six animals inoculated with the lowest dose of virus, one virus was transmitted to a single animal. However, this dose–response trend was not proportional across all dosage levels, and thus was not statistically significant, as animals receiving the highest virus inoculum did not differ from animals receiving the intermediate virus inoculum in the numbers of viruses leading to productive clinical infection.

Five animals did not become infected by the i.r. route despite 18 weekly inoculations (Fig. 1). Each of these animals did, however, become productively infected after a single i.v. inoculation of virus ( $2 \times 10^5$  vRNA copies). This i.v. dose was 300-fold lower than the maximum single i.r. dose ( $6 \times 10^7$ ) that each of the five animals had received and  $\sim 2,000$ -fold lower than the cumulative i.r. dose that each animal had received (Fig. 1 and Table I). Figs. 3 B and 4 B show NJ trees and *Highlighter* plots of *env* sequences from i.v.-infected animals CG71 and CP37. Even when animals were infected with multiple viruses, the progeny of transmitted/founder viruses could be identified with certainty in cases where two or more sequences were identical (e.g., CG71 *env* sequences corresponding to variants 1, 2, 6, 7 and 8 in Fig. 3 B), and with high likelihood if two or more sequences differed by only one or few nucleotides (e.g., CG71 *env* sequences corresponding to variants 3, 4, and 5 in Fig. 3 B). Identification of transmitted/founder viruses was less certain for individual sequences that were dispersed throughout the inoculum tree because such viruses could represent either transmitted variants (that replicated less efficiently) or unique recombinant viruses between two or more transmitted lineages. Thus, we made a conservative estimate that i.v. inoculation of animal CG71 resulted in productive infection by at least eight transmitted viruses. We reached a similar conclusion for animal CP37 (Fig. 4 B), for which there was evidence of productive infection by at least nine viruses. These are minimal estimates because as the number of transmitted viruses increases, the likelihood of sampling at least one of its progeny becomes increasingly dependent on the total number of sequences analyzed. For the five animals infected by the i.v. route, the number of transmitted/founder viruses that we identified ranged from 1 to  $>9$  with a median of 4 (Table I). Because each of these animals had not been infected by a cumulative i.r. dose of  $3.7\text{--}4.3 \times 10^8$  vRNA equivalents, but had become infected by  $2 \times 10^5$  vRNA equivalents given i.v., we could use these values together with the numbers of transmitted/founder viruses in each animal to estimate the relative efficiency of virus transmission by i.v. versus i.r. routes. We thus determined that i.v. transmission was 2,000–20,000-fold more efficient than i.r. transmission (Table I).

#### Detection of transmitted variants with minor representation

In some animals, the representation of viral lineages corresponding to transmitted/founder viruses was far from even.

For example, animal CT76 (Fig. S4) became infected by the i.r. route by four transmitted/founder viruses, two of which were represented only transiently in the ramp-up sample (variants 3 and 4). In CT76, the data can best be explained by variants 1 and 2 outgrowing variants 3 and 4, which were lost altogether from the sampled sequences by peak viremia. Macaque CG7V (Fig. 5) is a second example of an animal infected i.r. by five viruses, two represented by predominant *env* sequence lineages and three by single sequences (variants 3, 4, and 5). Macaque CP3C (Fig. 6) is a third example of an animal that was infected i.r. by at least three viruses, two of which were well represented and one that was represented by only a single ramp-up sequence (variant 3). We amplified an additional 220 *env* genes from ramp-up plasma viruses from this animal and identified just one additional member of this transmitted/founder lineage (unpublished data). Thus, this rare variant represented  $<1\%$  (2/269 sequences) of the replicating virus population. Notably, among the 269 sequences analyzed, we found no additional transmitted/founder virus lineages beyond the three depicted in Fig. 6. Animals CG7G and AK9F (Fig. S5) are two more examples of monkeys infected i.r. by multiple viruses, one or two of which were represented by lineages containing only single-sampled variants. Animals infected by the i.v. route were even more complicated because of the greater number of transmitted viruses overall (Figs. 3 B, 4 B, 7, S3, and S5). Compounding the unequal representation of sequences resulting from differences in replication efficiencies was the effect of recombination between viruses of two or more transmitted lineages. This is best seen in animal CG7V (Fig. 5), where recombinant viruses outnumbered one of the two principal transmitted lineages by nearly 3 to 1, and the minor variants by 20 to 1. Recombination was also observed in sequences from animals CG7G, CR54, CG71, and CG5G (Table I and Fig. S3).

#### Phylogenetic distribution of transmitted/founder viruses in the inocula

Sequences from all SIVmac251-infected animals and from the corresponding SIVmac251 inoculum are depicted in a single NJ tree (Fig. 7). Animals AV74, CG71, and CG5G were each inoculated by the i.v. route, and the  $>14$  transmitted/founder sequences that productively infected these animals are distributed widely throughout the tree. Several of these sequences differ from inoculum sequences by only 1 nt. Also represented in this NJ tree are sequences from seven animals infected by the i.r. route. Sequences from each of these animals are represented by one or more discrete low-diversity lineage whose consensus either matches an inoculum sequence (CP1W) or differs by only 1 or 2 nt (CT76, CR2A, and AH4X). Again, these transmitted/founder virus lineages are distributed widely throughout the tree. A similar pattern of inoculum and transmitted/founder SIVsmE660 *env* sequences is shown in Fig. S5. These findings highlight the diversity of *env* sequences in the SIVsmE660 and SIVmac251 inocula that are capable of mediating virus transmission and productive replication in macaques by i.v. or i.r. routes.

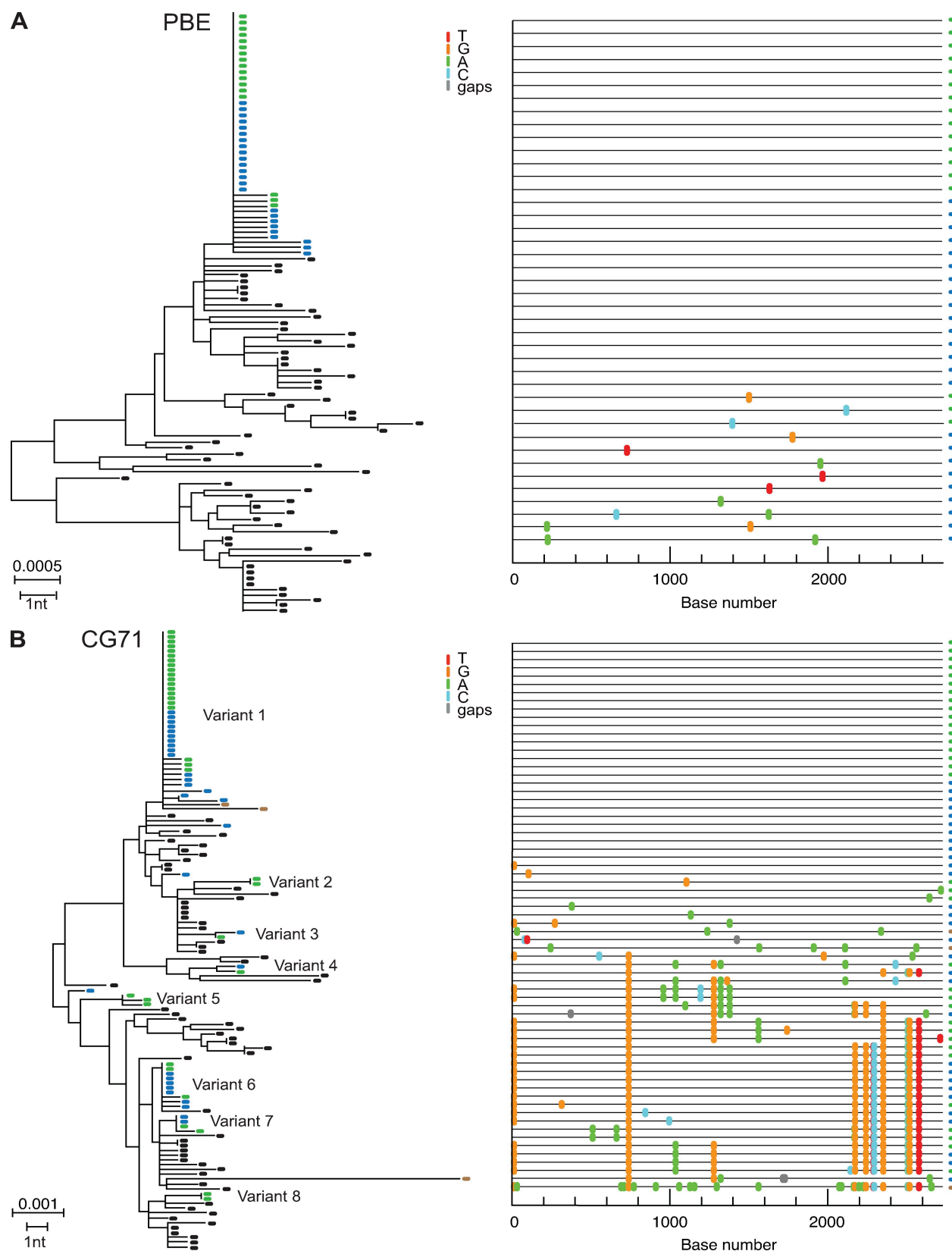


**Figure 3. Viral sequence diversity after i.r. or i.v. SIVmac251 infection.** (A) NJ and *Highlighter* analyses of sequences from i.r.-infected animal PBE at ramp-up (green symbols) or peak (blue symbols) viremia compared with inoculum sequences (black symbols). (B) i.v.-infected animal CG71. Brown labels indicate sequences with three or more APOBEC-mediated G-to-A mutations compared with consensus.

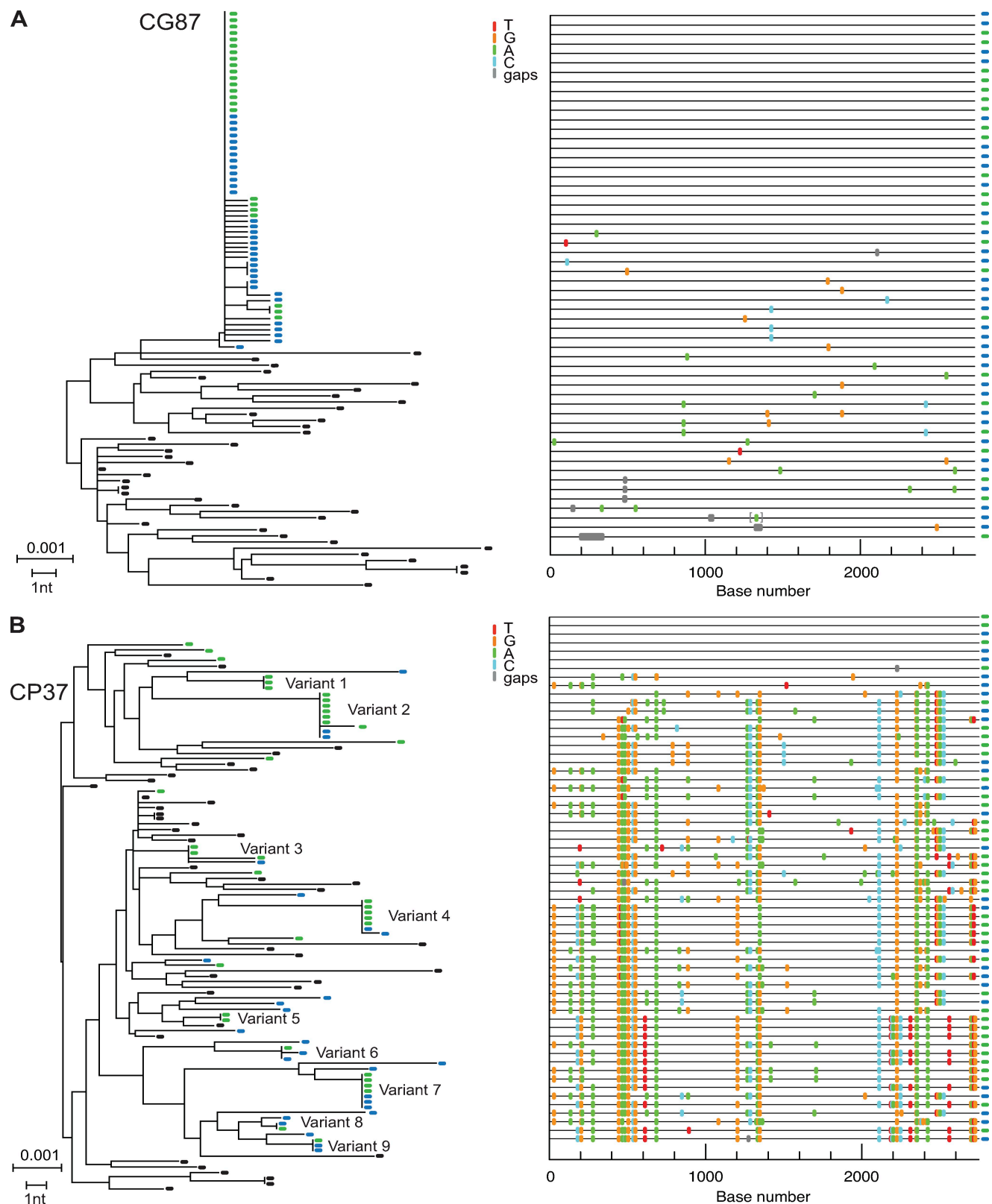


**Figure 4. Viral sequence diversity after i.r. or i.v. SIVsmE660 infection.** (A) NJ and *Highlighter* analyses of sequences from i.r.-infected animal CG87 at ramp-up (green symbols) or peak (blue symbols) viremia compared with inoculum sequences (black symbols). (B) i.v.-infected animal CP37. Nine transmitted/founder variant lineages are indicated, although additional minor variants and recombinants are also evident (see text). Bracket indicates a single-nucleotide insertion.

### Model analysis of SIV diversification

We previously described a mathematical model of HIV-1 replication and diversification in acute infection (5) using estimated parameters of HIV-1 generation time, reproductive ratio, and RT error rate and assuming that the initial virus replicates exponentially, infecting  $R_0$  new cells at each generation and diversifying under a model of evolution that assumes no selection, no back mutations, and a constant mutation rate across positions and lineages. Here, we applied this model to an analysis of 987 SIV *env* sequences and asked if measured parameters of virus diversification were consistent with the assumptions and predictions of this model. We examined data from all 18 animals. For those animals infected by more than one transmitted/founder virus, we selected a predominant lineage for analysis and excluded minor lineages and recombinant viruses. One animal (CP37) could not be analyzed for model conformation because it was infected by so many viruses that none formed a sufficiently predominant lineage (Fig. 4 B). A second animal (CP23) was included in the analysis, but with the caveat that sequences were obtained from a time point 2 wk after peak viremia, and 4–5 wk after infection, when rapid CTL selection is known to occur in

SIV-infected macaques (44, 45) and HIV-1-infected humans (5, 30, 35). For each animal, we obtained the frequency distribution of all intersequence Hamming distances (HDs; defined as the number of base positions at which two genomes differ) within a lineage and determined if it deviated from a Poisson model using a  $\chi^2$  goodness-of-fit test. We then determined whether or not the observed sequences evolved under a star phylogeny model (i.e., all evolving sequences are equally likely and all coalesce at the founder) in the expected time frame based on the known or estimated date of infection. Sequences from 16 of 17 animals exhibited an almost starlike phylogeny, the one exception being animal CP23 (Table I). Sequences from only 5 of 17 animals exhibited a Poisson distribution of base substitutions. The other 12 animals had sequences that showed enrichment for G-to-A hypermutation with APOBEC signatures (Table I). In 7 of these 12 animals, the evidence for hypermutation was restricted to a single sequence, whereas in 5 others, G-to-A hypermutation was enriched across multiple sequences. When these APOBEC-associated mutations were excluded from the analysis, a good fit to the Poisson model was restored for sequences from all 12 animals (Table I). 10 animals had rare sequences

**Table I.** Characterization of SIV transmission by intrarectal or intravenous inoculation

Subject	Initial dose	Cumulative dose before first + vRNA	Time to first + vRNA (wk)	Infection route	Peak viral load	No. of <i>env</i> seq. per animal	No. of identified transmitted variants	Percent max. <i>env</i> diversity	APOBEC-mediated G-to-A mutations	No. of APOBEC-mutated sequences	Intra-host recombination	Starlike phylogeny <sup>a</sup>	Poisson distribution <sup>a,b</sup>	Rectal barrier <sup>c</sup>
SIVsmE660-infected animals														
CG7V	$6 \times 10^7$	$1.2 \times 10^8$	2	i.r.	77,871,700	96	5	1.06	Yes	2	Yes	Yes	Yes	
CP3C	$6 \times 10^7$	$1.2 \times 10^8$	2	i.r.	1,112,900	49	3	0.84	Yes	1	No	Yes	Yes	
CG87	$6 \times 10^7$	$3.6 \times 10^8$	6	i.r.	479,543	56	1	0.15	No	–	N/A	Yes	Yes	
CG7G	$6 \times 10^6$	$6.0 \times 10^6$	1	i.r.	7,084,600	43	5	1.21	Yes	1	Yes	Yes	Yes	
AK9F	$6 \times 10^6$	$3.6 \times 10^7$	6	i.r.	140,795	35	4	1.43	No	–	No	Yes	Yes	
CP37	$6 \times 10^6$	$4.3 \times 10^8$	18	i.v.	94,394,600	62	>9	1.54	N/A <sup>d</sup>	N/A <sup>d</sup>	N/A <sup>d</sup>	N/A <sup>d</sup>	N/A <sup>d</sup>	>19,350
CP23 <sup>e</sup>	$6 \times 10^5$	$1.2 \times 10^6$	2	i.r.	74,000,000	37	1	0.33 <sup>e</sup>	Yes	1	N/A	No <sup>c</sup>	No <sup>c</sup>	
CR54	$6 \times 10^5$	$3.7 \times 10^8$	18	i.v.	1,968,800	29	4	1.26	Yes	1	Yes	Yes	Yes	7,400
SIVmac251-infected animals														
CP1W	$6 \times 10^7$	$6.0 \times 10^7$	1	i.r.	17,797,900	137	1	0.15	Yes	5	N/A	Yes	Yes	
CT76	$6 \times 10^7$	$6.0 \times 10^7$	1	i.r.	18,233,200	50	4	0.66	Yes	1	No	Yes	Yes	
PBE	$6 \times 10^7$	$3.0 \times 10^8$	5	i.r.	10,955,200	41	1	0.15	No	–	N/A	Yes	Yes	
CR2A	$6 \times 10^6$	$1.2 \times 10^7$	2	i.r.	4,130,600	46	1	0.07	No	–	N/A	Yes	Yes	
CR53	$6 \times 10^6$	$3.6 \times 10^7$	6	i.r.	6,341,200	30	1	0.15	Yes	1	N/A	Yes	Yes	
AV74	$6 \times 10^6$	$4.3 \times 10^8$	18	i.v.	18,690,000	71	1	0.18	Yes	3	N/A	Yes	Yes	2,150
AH4X	$6 \times 10^5$	$2.5 \times 10^8$	16	i.r.	2,611,600	23	2	0.59	No	–	No	Yes	Yes	
CG71	$6 \times 10^5$	$3.7 \times 10^8$	18	i.v.	8,857,400	67	>8	0.73	Yes	3	Yes	Yes	Yes	>14,800
CG5G	$6 \times 10^5$	$3.7 \times 10^8$	18	i.v.	12,938,400	71	4	0.81	Yes	2	Yes	Yes	Yes	7,400
AV66	$6 \times 10^5$	$6.7 \times 10^7$	13	i.r.	4,858,300	44	1	0.07	Yes	1	N/A	Yes	Yes	

<sup>a</sup>If infected with more than one variant, the major lineages were examined for a starlike phylogeny and Poisson distribution of substitutions excluding APOBEC-mediated changes.

<sup>b</sup>APOBEC-mutated sequences excluded.

<sup>c</sup>Rectal barrier was calculated by dividing the cumulative i.r. dose by the i.v. dose multiplied by the number of transmitted viruses.

<sup>d</sup>Not applicable; too many variants to quantify.

<sup>e</sup>Sampled 2 wk after peak viral load.



that exhibited shared mutations. For example, CG87 (Fig. 4 A) contained 3 of 56 sequences that shared one nucleotide polymorphism, 3 other sequences that shared a different polymorphism, and 3 additional sequences that shared 1 or 2 still different polymorphisms. Animal CT76 (Fig. S4) had 3 of 50 sequences that shared a single-nucleotide polymorphism. Based on the temporal appearance and patterns of these mutations and a mathematical modeling estimate of the expected frequency of sequences having one or more shared mutations in a gene the size of *env* (5, 30), we could explain these rare sublineages as resulting from stochastic mutations generated shortly after transmission. In contrast, sequences from animal CP23 obtained 2 wk after peak viremia contained a far higher number of shared mutations than did sequences from any other animal. Most of these shared mutations were narrowly confined to a short stretch of 19 nt. Thus, CP23 sequences severely violated model predictions for random variation as a consequence of early selection, similar to findings we made in HIV-1-infected humans who were sampled within 2 wk

after peak viremia (5, 30, 35). Sequences from animals infected by more than one virus also violated model expectations for a Poisson distribution and starlike phylogeny of mutations, but did conform to the model when *env* sublineages were analyzed individually (Table I).

Table II summarizes model estimates of time to a MRCA sequence in each animal. For this analysis, we used Bayesian (46, 47) and Poisson-based (5) approaches (Supplemental materials and methods). Bayesian and Poisson estimates of a MRCA of sequences in most animals were consistent with the known or estimated days since infection. This is best seen in animal CP1W, where 137 sequences (69 from ramp-up and 68 from peak viremia) were analyzed, and for which both the duration of infection before plasma sampling and the *env* sequence of the transmitted virus were known with certainty. Here, we observed the Poisson model estimate of a MRCA for ramp-up sequences to be 6 d (confidence interval [CI] 1–10 d) and for peak viremia sequences to be 10 d (CI 5–15 d). Bayesian calculations used sequence information from both time points to

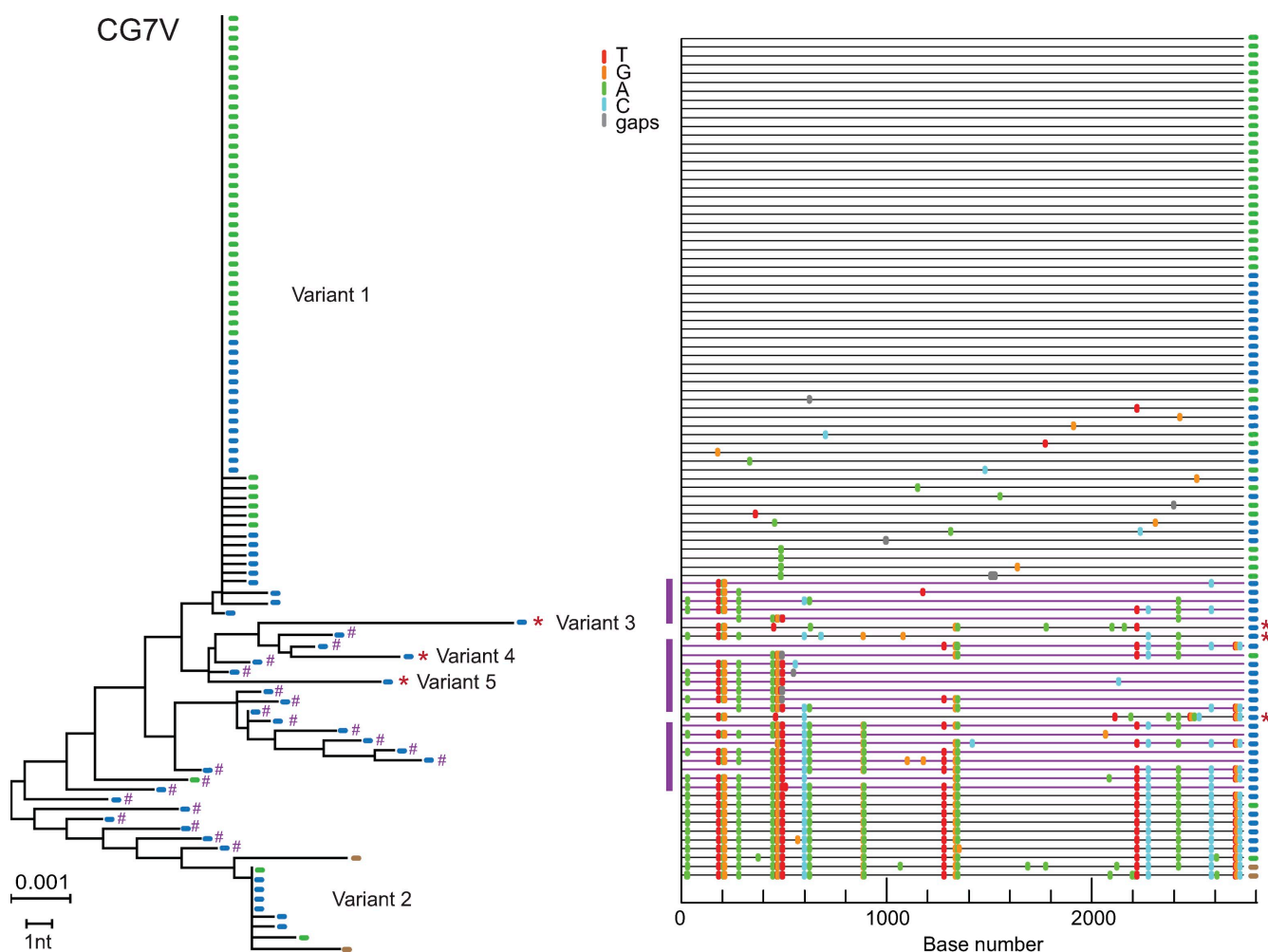


**Figure 5.** i.r. transmission of five viruses, followed by extensive recombination. NJ and Highlighter plots from animal CG7V at ramp-up (green symbols) or peak (blue symbols) viremia with recombinant sequences labeled in purple (#) and minor transmitted/founder viral variants 3, 4, and 5 in red (\*). Brown labels indicate sequences with three or more APOBEC-mediated G-to-A mutations compared with consensus.

estimate a coalescent MRCA for the peak viremia sequences of 12 d (CI 8–20 d). Thus, Poisson and Bayesian estimates concurred closely with each other and with the known duration of infection of the animal. Model estimates of time to a MRCA were not close to the known duration of infection for animal CP23, which was sampled 2 wk after peak viremia when there was evidence of strong selection for mutations. Selected mutations are nonrandom and violate model assumptions. For CP23, the Bayesian estimate for a MRCA was 50 d (CI 28–84 d) and the Poisson estimate was 55 d (CI 47–62 d), exceeding the known duration of infection of 28–35 d. For three animals (CR2A, CG5G, and AV66), the Poisson estimates and CIs of days since a MRCA were less than the known or estimated duration of virus infection, possibly because of purifying selection, differences in virus replication parameters such as virus generation time, RT error frequency or  $R_0$  compared with model assumptions, or a sampling effect.

## DISCUSSION

Previously, we developed a conceptual framework, mathematical model, and empirical dataset of HIV-1 *env* sequences that together suggested transmitted/founder viruses respon-

sible for productive clinical infection could be identified by phylogenetic inference in acutely infected subjects (5). A key inference from this model and the supporting HIV-1 sequence datasets (5, 28–35) is that between the time the first cell is infected in the mucosa or submucosa and the time peak viremia is reached  $\sim 3$ –5 wk later (eclipse phase and Fiebig stages I and II), viruses diversify essentially randomly with little or no evidence of biological selection. This is in contrast to the period immediately thereafter (Fiebig stages III–V), when evidence of strong CTL selection generally becomes apparent (5, 30, 35). Using pyrosequencing technologies that allow for a more extensive sampling of sequences, we have recently found evidence of CTL selection beginning as early as Fiebig stage II (unpublished data). A second key inference from the model and HIV-1 datasets is that by analyzing *env* sequence diversity among 30–50 plasma viruses sampled near the time of peak viremia, sufficient sequence information is available to allow for an unambiguous phylogenetic inference of transmitted/founder virus(es) weeks earlier. This conclusion is based on power calculations that provide 95% confidence limits for detecting minor sequence variants and the empirical observation

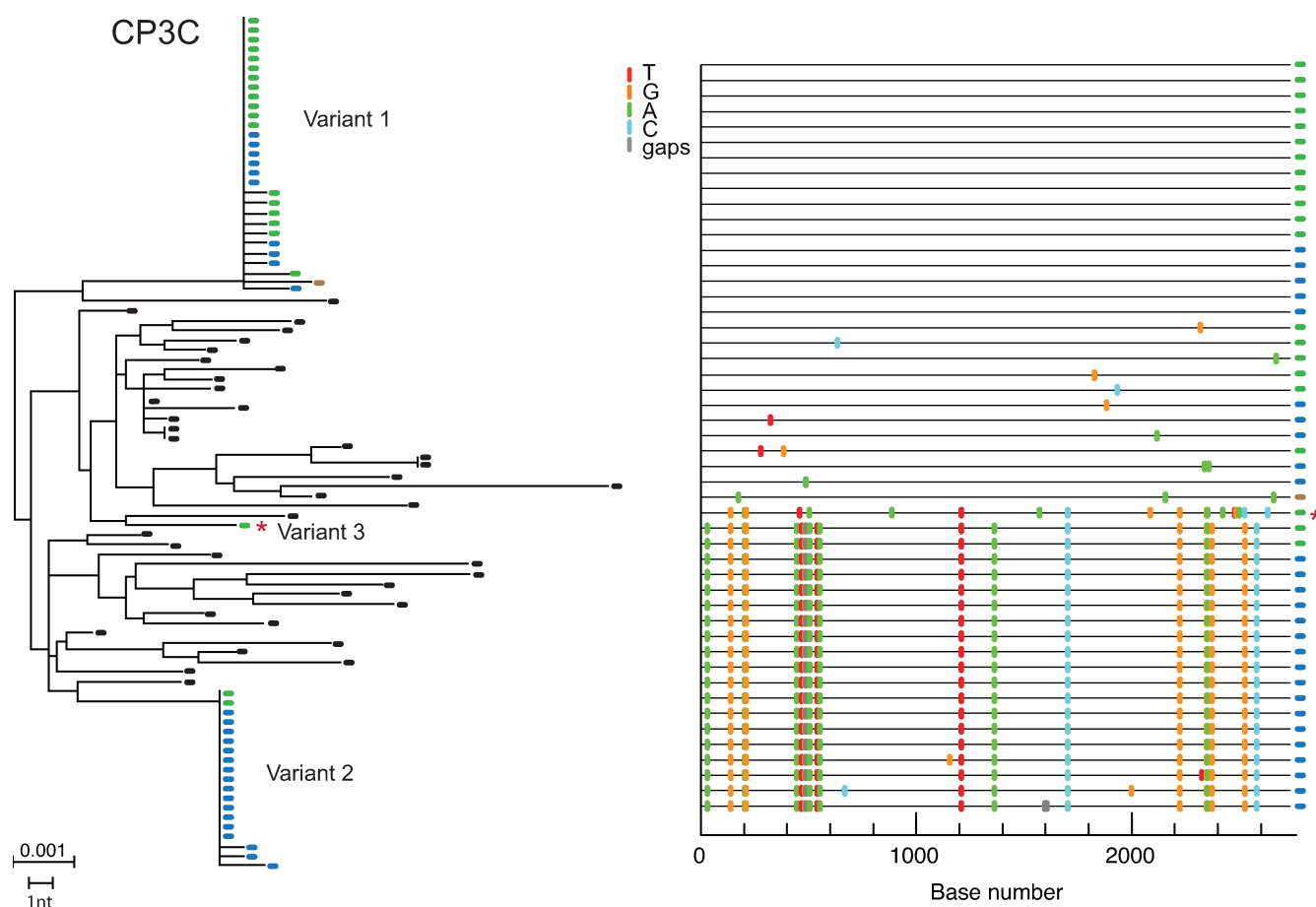


**Figure 6. Unequal representation of transmitted viruses.** Transmitted variants 1 and 2 in animal CP3C are well represented at ramp-up (green symbols) and peak (blue symbols) viremia compared with a third transmitted variant (red asterisk) that is represented by only a single sequence at ramp-up. Inoculum sequences are indicated by black symbols.

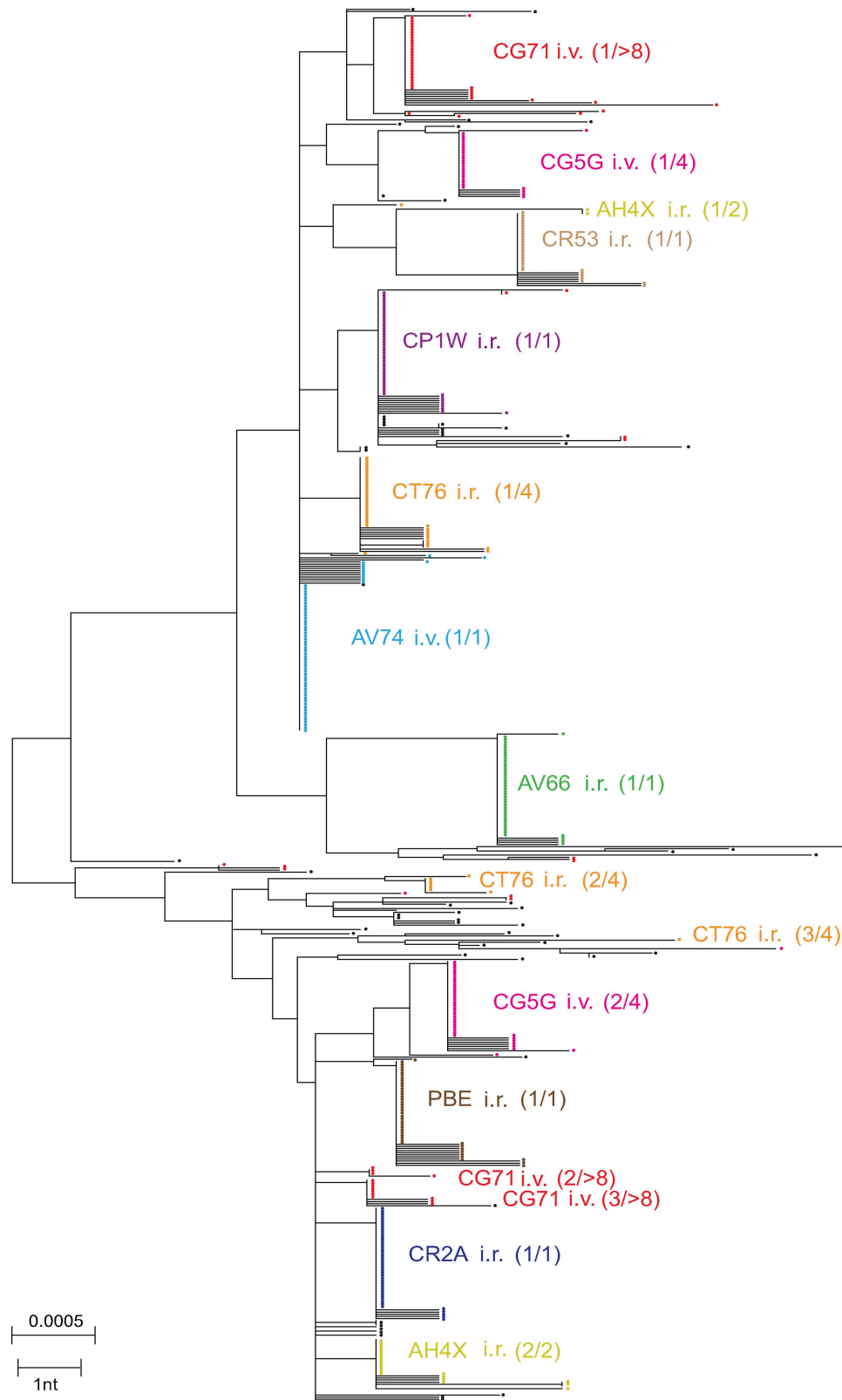


**Figure 7. Composite SIVmac251 tree from i.r.- and i.v.-infected animals.** The NJ tree depicts numerous transmitted/founder virus lineages distributed throughout a diverse set of inoculum sequences (black symbols). Most i.r.- or i.v.-transmitted viruses are represented by discrete, low-diversity lineages. Animal designation, route of infection, and numbers of transmitted viruses are indicated.

that between transmission and peak viremia (Fiebig stage II), it is uncommon to find sequences that exhibit shared polymorphisms resulting from immune selection (5, 30); when this does occur, it is necessary to analyze sequential samples to distinguish transmitted/founder sequences from selected mutants. In this study, we tested our model assumptions and inferences directly in the SIV-macaque infection model where experimental conditions, including the composition of the virus inoculum and the interval between virus inocu-

lation and plasma sampling for *env* sequence analysis, could be better defined (Fig. 1).

Fig. 2 illustrates ramp-up and peak viremia plasma vRNA sequences in animal CP1W after a typical i.r. infection by SIVmac251 and demonstrates many of the salient features of the SGA-direct sequence analysis. After elimination of five sequences that contained APOBEC-related G-to-A hypermutations, the remaining 132 *env* sequences conformed to a star-like phylogeny and exhibited a Poisson

**Table II.** Model analysis of early SIV evolution in SIVsmE660- and SIVmac251-infected rhesus macaques

Subject	Sample time	Infection route	No. of sequences examined	Max. HD	BEAST estimated days since MRCA (95% CI)	Poisson estimated days since MRCA (95% CI)	$\lambda^a$	SD <sup>b</sup>	Goodness of fit p-value <sup>c</sup>
SIVsmE660-infected animals									
CG7V	Ramp-up	i.r.	39	2		6 (3,8)	0.308	0.082	0.584
	Peak	i.r.	23	4	12 (8,19)	13 (7,20)	0.762	0.190	0.840
CP3C	Ramp-up	i.r.	19	3		13 (6,20)	1.053	0.189	0.913
	Peak	i.r.	10	3	17 (10,29)	11 (3,18)	1.000	0.220	0.815
CG87	Ramp-up	i.r.	23	4		15 (8,22)	0.854	0.210	0.663
	Peak	i.r.	33	4	20 (12,34)	23 (18,28)	1.311	0.156	0.220
CG7G	Ramp-up	i.r.	18	2		12 (6,17)	0.667	0.159	0.317
	Peak	i.r.	17	3	16 (10,27)	13 (6,20)	0.750	0.209	0.865
AK9F	Peak	i.r.	19	4	12 (2,43)	14 (7,22)	0.807	0.216	0.886
CP37 <sup>d</sup>	–	–	–	–	–	–	–	–	–
CP23	2 wk after peak	i.r.	37	8	50 (28,84)	55 (47,62)	3.129	0.221	0.038
CR54	Peak	i.v.	17	3	14 (2,52)	12 (5,20)	0.706	0.206	0.874
SIVmac251-infected animals									
CP1W	Ramp-up	i.r.	69	4		6 (1,10)	0.316	0.123	0.654
	Peak	i.r.	68	4	12 (8,20)	10 (5,15)	0.552	0.143	0.906
CT76	Ramp-up	i.r.	20	3		17 (10,24)	0.968	0.208	0.809
	Peak	i.r.	22	3	16 (7,34)	7 (1,12)	0.455	0.153	0.701
PBE	Ramp-up	i.r.	17	2		6 (2,11)	0.353	0.139	0.646
	Peak	i.r.	24	4	13 (8,21)	12 (7,17)	0.667	0.142	0.211
CR2A	Ramp-up	i.r.	19	3		2 (0,5)	0.105	0.077	0.750
	Peak	i.r.	27	2	8 (7,14)	5 (2,9)	0.296	0.101	0.637
CR53	Peak	i.r.	30	4	12 (3,58)	12 (6,18)	0.667	0.166	0.478
AV74	Ramp-up	i.v.	35	3		5 (2,9)	0.284	0.103	0.703
	Peak	i.v.	36	3	12 (8,20)	14 (8,20)	0.778	0.174	0.621
AH4X	Peak	i.r.	21	6	11 (2,80)	10 (4,16)	0.561	0.173	0.894
CG71	Ramp-up	i.v.	22	2		7 (2,11)	0.364	0.124	0.617
	Peak	i.v.	16	5	14 (8,25)	17 (8,27)	0.983	0.279	0.630
CG5G	Ramp-up	i.v.	24	4		6 (1,11)	0.333	0.137	0.655
	Peak	i.v.	17	4	9 (7,14)	6 (2,11)	0.353	0.136	0.646
AV66	Ramp-up	i.r.	20	2		5 (1,9)	0.300	0.115	0.657
	Peak	i.r.	24	2	9 (7,28)	3 (0,6)	0.167	0.082	0.713

<sup>a</sup>Mean of best fitting Poisson distribution defined by the free parameter  $\lambda$ .

<sup>b</sup>SD of  $\lambda$  obtained by using jackknife.

<sup>c</sup>P < 0.05 indicates that sequences deviate significantly from a Poisson distribution.

<sup>d</sup>Not applicable; too many variants to identify major lineage.

distribution of nucleotide substitutions. At 7 d after infection, 59 of 67 (88%) sequences were identical, and at 14 d after infection, 51 of 65 (78%) sequences were identical. This degree of early SIV *env* sequence homogeneity followed by a decline in sequence identity from 88% to 78% over a 7-d period is strikingly similar to findings made in humans acutely infected by HIV-1 and conforms closely to model projections previously reported (5). Bayesian and Poisson estimations of days from a MRCA were consistent with the known duration of infection in this animal (Table II), and an unambiguous transmitted/founder SIVmac251 sequence could be inferred from the consensus of sequences at ramp-up and peak viremia time points. The validity of this conclusion was confirmed by an analysis of the SIVmac251 inoculum (Fig. 2), where four *env* sequences were found that were identical to the transmitted/founder *env* sequence in animal CP1W. This result shows that a transmitted SIV genome can be identified in an inoculum, and can then be traced across the rectal mucosa of the newly infected host and through the period of massive virus expansion in gut-associated and peripheral lymphoid tissues that leads ultimately to peak plasma viremia (2, 3, 19, 45, 48–52). Recent studies in human transmission pairs where identical HIV-1 *env* sequences were identified in donor and recipient plasma after sexual HIV-1 transmission corroborate these findings (28, 33).

Despite the identification of one or more transmitted/founder *env* genes in all 18 animals studied, we note that the detection of such discrete, low-diversity SIV lineages (representing the progeny of transmitted/founder viruses) does not mean that these represented the *only* viruses transmitted across the mucosal epithelium. It is possible that additional viruses were transmitted across the mucosa, but went undetected because of limited sampling, stochastic infection events, abortive infection, defective viruses, innate immune responses, unequal replication rates of competing virus lineages, or virus compartmentalization (26, 53–56). The same is true for HIV-1-infected humans where determinations of numbers of transmitted/founder viruses correspond to minimum estimates (5). With these caveats in mind, we obtained minimum estimates of the numbers of transmitted viruses leading to productive clinical infection in the 18 macaque monkeys infected by i.r. or i.v. routes. The results are depicted in Fig. 1 and are summarized in Table I, where the cumulative virus dose administered to each animal before the first positive plasma vRNA result is also listed. The findings show that rectal inoculation of SIV led to productive infection by a minimum of 1–5 viruses (median = 1). Five animals did not become infected even after 18 rectal inoculations. Each of these animals did become infected after a single intravenous inoculation with a dose of virus 300-fold less than the highest individual i.r. dose. These animals were productively infected by a minimum of 1–9 viruses (median = 4). After accounting for differences in the cumulative i.r. virus exposure of these animals and the minimum estimates of the numbers of transmitted viruses, i.v. transmission efficiency was calculated to

exceed rectal transmission efficiency by 2,000–20,000-fold. This finding is consistent with the demonstrably higher risk of HIV-1 transmission resulting from i.v. exposure to contaminated blood products than from sexual exposures in humans (4, 57, 58) and comparable findings in SIV-inoculated monkeys (26, 55, 56).

One peculiarity in the findings illustrated in Fig. 1 is the observation that while i.r. inoculation with the two higher viral doses resulted in greater numbers of transmitted viruses compared with the lowest dose, this relationship was not proportional across all three virus dose levels. For example, there were animals in the highest dose group (e.g., CP1W and CG87) that were infected by a single virus and other animals in the middle dose group (e.g., AK9F and CG7G) that were infected by four or five viruses. This observation in macaques has an interesting parallel in humans where two recent studies of mucosal HIV-1 infection revealed that transmission of multiple viruses did not follow an expected Poisson distribution of independent, low-frequency events (5, 31). In those studies, the proportion of individuals who acquired more than one HIV-1 variant was higher than could be plausibly explained by known rates of HIV-1 sexual transmission (4, 57, 58). Moreover, the proportion of individuals who became infected by three or more viruses was disproportionately higher still. At present, there is no satisfactory biological explanation in humans or macaques for the observed non-Poisson distribution of infection events, although mucosal tears, ulceration, inflammation, or infection by multiply infected cells or virus aggregates are possibilities (31, 33).

Three features of SIV mucosal transmission that differ from HIV-1 mucosal transmission are a shorter eclipse period for SIV, a higher frequency of G-to-A hypermutated SIV sequences, and a higher frequency of detection of minor transmitted SIV variants (identified as rare variant sequences in ramp-up or peak viremia samples). Although the design of this study, which included weekly i.r. inoculations of virus and weekly plasma sampling, was not intended to provide a precise estimate of the duration of the eclipse period, we could determine an upper boundary for the eclipse phase in animals CP1W, CT76, CG7G, and AV66. In each case, it was < 7 d. This is substantially shorter than the average eclipse phase of HIV-1 in humans of ~10–14 d, and which may exceed 21 d (for review see [5]). Potential explanations for this difference include an ~10-fold lower plasma and extracellular fluid volume in macaques into which virus can distribute, together with a higher exponential growth rate and reproductive ratio for SIV compared with HIV-1 (27, 59). A second difference between SIV and HIV-1 mucosal transmission was a substantially higher frequency of detection of SIV sequences with APOBEC-related G-to-A hypermutation in the acute and early infection period. For example, SIV *env* sequences from 12 of 18 macaques initially did not conform to a Poisson model of random virus evolution because of APOBEC hypermutation, whereas HIV-1 *env* sequences from only 13 of 81 humans (5) deviated

from the model because of APOBEC hypermutation ( $P < 0.0001$ ; Fisher's exact test). In a separate study, we also found examples of excessive G-to-A hypermutation of SIV in mucosally infected animals in the acute infection period (60). Heterogeneity of *vif* sequences in the SIV inoculum and in the transmitted/founder viruses that arise from them, or a greater evolutionary mismatch between SIVsm (SIV-mac) Vif proteins and the Indian rhesus macaque APOBEC, compared with SIVcpz (HIV-1) Vif proteins and human APOBEC (61), may contribute to these differences. A third difference we found between mucosal SIV and HIV-1 infection was in the numbers of minor virus variants detected in ramp-up or peak viremia plasma samples. Rare virus variants were found in 5 of 13 mucosally infected macaques compared with 4 of 98 human subjects (5) ( $P = 0.001$ ; Fisher's exact test). This difference may be caused by the fact that macaques were inoculated i.r. with higher titers of virus having greater diversity in replicative potential (as a consequence of in vitro propagation) compared with virus that is transmitted sexually in humans (4, 58, 62, 63) or to later sampling of humans (5).

In summary, this study demonstrates that i.r. infection of rhesus macaques recapitulates at a biological and molecular level many of the features of human HIV-1 mucosal transmission. When the SIV inoculum is sufficiently low, mucosal transmission is infrequent and dose related; higher SIV doses, like higher HIV-1 titers in humans (58, 62–64), are associated with higher transmission rates. The numbers of transmitted/founder viruses yielding productive clinical infection in mucosally infected humans (generally 1–5; median = 1; [5, 28, 29, 31–35]) and macaques (1–5; median = 1) were low, reflecting a substantial bottleneck in mucosal transmission in both species. In neither humans nor macaques did the numbers of transmitted viruses after mucosal exposure correspond to a Poisson distribution of independent, low-probability events (5, 31). Diversification of SIV and HIV-1 before peak viremia was essentially random and without evidence of immune selection; between peak viremia and 2 wk hence, there was evidence of strong CTL selection for escape variants in both macaques and humans (Fig. S2) (5, 30, 35, 44, 45). In acute SIV and HIV-1 infection, interlineage recombination was common (5). Further studies are needed to elucidate the precise nature of the bottleneck to mucosal transmission of SIV and HIV-1 and how it compares in rectal versus vaginal transmission. It will also be important to determine if the identification and enumeration of transmitted/founder viruses in humans or macaques can augment in a meaningful way the analysis of vaccine-mediated protection or enhancement of infection. Finally, we suggest that the analysis of full-length transmitted/founder viruses and their progeny in the SIV-macaque infection model can provide a uniquely informative view of the composite selection pressures shaping virus evolution beginning at or near the moment of transmission and extending to setpoint viremia, as shown recently for HIV-1 (30).

## MATERIALS AND METHODS

**Study animals.** Frozen ( $-70^{\circ}\text{C}$ ) plasma specimens collected from 18 adult rhesus macaques (*Macaca mulatta*) as part of a previous study of low-dose intrarectal SIV inoculation (41) were analyzed. The SIVmac251 and SIVsmE660 inoculum stocks and the inoculation procedures were previously described in detail (41). All animals were maintained in an Association for Assessment and Accreditation of Laboratory Animal Care-accredited institution and with the approval of the Animal Care and Use Committees of the National Institutes of Health and Harvard Medical School (41).

**Viral RNA extraction and cDNA synthesis.** From each plasma specimen,  $\sim 20,000$  viral RNA copies were extracted using the QIAamp Viral RNA Mini kit (QIAGEN). RNA was eluted and immediately subjected to cDNA synthesis. Reverse transcription of RNA to single-stranded cDNA was performed using SuperScript III reverse transcription according to manufacturer's recommendations (Invitrogen). In brief, each cDNA reaction included  $1 \times$  RT buffer, 0.5 mM of each deoxynucleoside triphosphate, 5 mM dithiothreitol, 2 U/ml RNaseOUT (RNase inhibitor), 10 U/ml of SuperScript III reverse transcription, and 0.25 mM antisense primer SIVsm/macEnvR1 5'-TGTAATAAATCCCTTCCAGTCCCCC-3' (nt 9454–9479 in SIVmac239). The mixture was incubated at  $50^{\circ}\text{C}$  for 60 min, followed by an increase in temperature to  $55^{\circ}\text{C}$  for an additional 60 min. The reaction was then heat-inactivated at  $70^{\circ}\text{C}$  for 15 min and treated with 2 U of RNase H at  $37^{\circ}\text{C}$  for 20 min. The newly synthesized cDNA was used immediately or frozen at  $-80^{\circ}\text{C}$ .

**SGA.** cDNA was serially diluted and distributed among wells of replicate 96-well plates so as to identify a dilution where PCR-positive wells constituted  $<30\%$  of the total number of reactions, as previously described (5, 35). At this dilution, most wells contain amplicons derived from a single cDNA molecule. This was confirmed in every positive well by direct sequencing of the amplicon and inspection of the sequence for mixed bases (double peaks), which would be indicative of priming from more than one original template or the introduction of PCR error in early cycles. Any sequence with mixed bases was excluded from further analysis. PCR amplification was performed in the presence of  $1 \times$  High Fidelity Platinum PCR buffer, 2 mM  $\text{MgSO}_4$ , 0.2 mM of each deoxynucleoside triphosphate, 0.2  $\mu\text{M}$  of each primer, and 0.025 U/ $\mu\text{l}$  Platinum *Taq* High Fidelity polymerase in a 20- $\mu\text{l}$  reaction (Invitrogen). First round PCR primers included sense primer SIVsm/macEnvF1 5'-CCTCCCCCTCCAGGACTAGC-3' (nt 6127–6146 in SIVmac239) and antisense primer SIVsm/macEnvR1 5'-TGTAATAAATCCCTTCCAGTCCCCC-3' (nt 9454–9479 in SIVmac239), which generated an  $\sim 3.3$ -kb amplicon. PCR was performed in MicroAmp 96-well reaction plates (Applied Biosystems) with the following PCR parameters: 1 cycle of  $94^{\circ}\text{C}$  for 2 min, 35 cycles of a denaturing step of  $94^{\circ}\text{C}$  for 15 s, an annealing step of  $55^{\circ}\text{C}$  for 30 s, and an extension step of  $68^{\circ}\text{C}$  for 4 min, followed by a final extension of  $68^{\circ}\text{C}$  for 10 min. Next, 2  $\mu\text{l}$  from first-round PCR product was added to a second-round PCR reaction that included the sense primer SIVsmEnvF2 5'-TATGATAGACATGGAGACACCCTTG-AAGGAGC-3' (nt 6292–6323 in SIVmac239) or SIVmacEnvF2 5'-TAT-AATAGACATGGAGACACCCTTGAGGGAGC-3' (nt 6292–6323 in Mac239) and antisense primer SIVsmEnvR2 5'-ATGAGACATRTC-TATTGCCAATTTGTA-3' (nt 9413–9439 in SIVmac239). The second-round PCR reaction was performed under the same conditions used for first-round PCR, but with a total of 45 cycles. Amplicons were inspected on precast 1% agarose E-gels 96 (Invitrogen). All PCR procedures were performed under PCR clean room conditions using procedural safeguards against sample contamination, including prealiquoting of all reagents, use of dedicated equipment, and physical separation of sample processing from pre- and post-PCR amplification steps.

**DNA sequencing.** Env gene amplicons were directly sequenced by cycle-sequencing using BigDye terminator chemistry and protocols recommended by the manufacturer (Applied Biosystems). Sequencing reaction products were analyzed with an ABI 3730xl genetic analyzer (Applied Biosystems). Both DNA



strands were sequenced using partially overlapping fragments. Individual sequence fragments for each amplicon were assembled and edited using the Sequencher program 4.7 (Gene Codes). Inspection of individual chromatograms allowed for the confirmation of amplicons derived from single versus multiple templates. The absence of mixed bases at each nucleotide position throughout the entire *env* gene was taken as evidence of SGA from a single vRNA/cDNA template. This quality control measure allowed us to exclude from the analysis amplicons that resulted from PCR-generated in vitro recombination events or *Taq* polymerase errors and to obtain individual *env* sequences that proportionately represented those circulating in vivo in SIV virions.

**Sequence alignments.** All alignments were initially made with Clustal W (65). Consensus sequences were generated for the sequence set from each individual. The full alignment for SIVsmE660 and SIVmac251 is available at [www.hiv.lanl.gov/content/sequence/hiv/user\\_alignments/keeleSIV](http://www.hiv.lanl.gov/content/sequence/hiv/user_alignments/keeleSIV). All 1090 *env* sequences from ramp-up and peak viremia and from the inoculum stocks were deposited in GenBank/EMBL/DBJ (available at accession nos. FJ578007–FJ579096).

**Env diversity analysis.** A total of 987 full-length SIV *env* genes of plasma virions from 18 animals (median of 48 per animal; range 23–137) were sequenced. Power calculations indicated that with a sample of 48 sequences, we could be 95% confident not to miss a transmitted variant that comprised at least 5% of the total virus population (5). Similarly, with a sample size between 23 and 137, we could be 95% confident not to miss a variant comprising between 3 and 12% of the total virus population. Out of 987 total sequences, 26 were excluded from further analysis because of overt APOBEC-associated G-to-A hypermutation (defined as three or more G-to-A substitutions in APOBEC signature motifs). We next analyzed sequences for maximum *env* diversity, and then by NJ phylogenies and *Highlighter* plots ([www.hiv.lanl.gov](http://www.hiv.lanl.gov)). For each animal having sequences that comprised more than one low-diversity lineage, we identified the lineage with the greatest sequence representation for subsequent analysis. Pairwise HD (defined as the number of base positions at which the two genomes differ, excluding gaps) were determined for each transmitted/founder lineage. The inoculum stocks of SIVsmE660 and SIVmac251 were evaluated for maximum *env* diversity and by NJ phylogenies and *Highlighter* plots.

**Hypermutated samples.** Enrichment for APOBEC mutations violates the assumption of constant mutation rate across positions, as the editing performed by these enzymes is base and context sensitive. Enrichment for mutations with APOBEC signatures was assessed using Hypermut 2.0 ([www.hiv.lanl.gov](http://www.hiv.lanl.gov)).

**Viral recombination.** Recombination analysis was performed by visual inspection of *Highlighter* trees and confirmed by RAP ([www.hiv.lanl.gov](http://www.hiv.lanl.gov)), GARD (66), or Recco (67) recombination identification tools.

**Model analyses.** Detailed descriptions of the mathematical models of early sequence evolution, star phylogeny determination, estimates of viral fitness, and power calculations for estimating the likelihood of detecting transmitted *env* variants with minor representation are provided elsewhere (5). Bayesian (46, 47) and Poisson analyses (5) are described in the Supplemental materials and methods.

**Statistical analysis.** We used the R software package, Version 2.8.0, to perform hypothesis tests.

**Online supplemental material.** Bayesian and Poisson analyses are described in the Supplemental materials and methods. Fig. S1 shows NJ trees and *Highlighter* plots of *env* sequences from the SIVsmE660 and SIVmac251 inocula. Fig. S2 shows viral *env* sequence diversity 2 wk after peak viremia in an i.r.-infected animal CP23. Fig. S3 shows i.v. transmission of four viruses, followed by recombination in animal CG5G. Fig. S4 shows i.r. transmission of four viruses in animal CT76. Fig. S5 shows a composite NJ tree of SIVsmE660 sequences from the inoculum and from i.r.- and i.v.-infected animals. Online supplemental material is available at <http://www.jem.org/cgi/content/full/jem.20080831/DC1>.

We thank D. McPherson and B. Cochran for technical assistance; sequencing core facilities of the UAB CFAR; and J. White for manuscript preparation.

This work was supported by the Center for HIV/AIDS Vaccine Immunology and by grants from the National Institutes of Health (AI67854 and AI27767), the Bill and Melinda Gates Foundation (#37874), and the American Foundation for AIDS Research (106997-3).

The authors have no conflicting financial interests.

Submitted: 18 December 2008

Accepted: 3 April 2009

## REFERENCES

- Chun, T.W., D. Engel, M.M. Berrey, T. Shea, L. Corey, and A.S. Fauci. 1998. Early establishment of a pool of latently infected, resting CD4(+) T cells during primary HIV-1 infection. *Proc. Natl. Acad. Sci. USA*. 95:8869–8873.
- Haase, A.T. 2005. Perils at mucosal front lines for HIV and SIV and their hosts. *Nat. Rev. Immunol.* 5:783–792.
- Pope, M., and A.T. Haase. 2003. Transmission, acute HIV-1 infection and the quest for strategies to prevent infection. *Nat. Med.* 9:847–852.
- Shattock, R.J., and J.P. Moore. 2003. Inhibiting sexual transmission of HIV-1 infection. *Nat. Rev. Microbiol.* 1:25–34.
- Keele, B.F., E.E. Giorgi, J.F. Salazar-Gonzalez, J.M. Decker, K.T. Pham, M.G. Salazar, C. Sun, T. Grayson, S. Wang, H. Li, et al. 2008. Identification and characterization of transmitted and early founder virus envelopes in primary HIV-1 infection. *Proc. Natl. Acad. Sci. USA*. 105:7552–7557.
- Grobler, J., C.M. Gray, C. Rademeyer, C. Seoighe, G. Ramjee, S.A. Karim, L. Morris, and C. Williamson. 2004. Incidence of HIV-1 dual infection and its association with increased viral load set point in a cohort of HIV-1 subtype C-infected female sex workers. *J. Infect. Dis.* 190:1355–1359.
- Long, E.M., H.L. Martin Jr., J.K. Kreiss, S.M. Rainwater, L. Lavreys, D.J. Jackson, J. Rakwar, K. Mandaliya, and J. Overbaugh. 2000. Gender differences in HIV-1 diversity at time of infection. *Nat. Med.* 6:71–75.
- Poss, M., H.L. Martin, J.K. Kreiss, L. Granville, B. Chohan, P. Nyange, K. Mandaliya, and J. Overbaugh. 1995. Diversity in virus populations from genital secretions and peripheral blood from women recently infected with human immunodeficiency virus type 1. *J. Virol.* 69:8118–8122.
- Ritola, K., C.D. Pilcher, S.A. Fiscus, N.G. Hoffman, J.A. Nelson, K.M. Kittrinos, C.B. Hicks, J.J. Eron Jr., and R. Swanstrom. 2004. Multiple V1/V2 *env* variants are frequently present during primary infection with human immunodeficiency virus type 1. *J. Virol.* 78:11208–11218.
- Sagar, M., E. Kirkegaard, E.M. Long, C. Celum, S. Buchbinder, E.S. Daar, and J. Overbaugh. 2004. Human immunodeficiency virus type 1 (HIV-1) diversity at time of infection is not restricted to certain risk groups or specific HIV-1 subtypes. *J. Virol.* 78:7279–7283.
- Wolf, T.F., G. Zwart, M. Bakker, and J. Goudsmit. 1992. HIV-1 genomic RNA diversification following sexual and parenteral virus transmission. *Virology*. 189:103–110.
- Wolinsky, S.M., C.M. Wike, B.T. Korber, C. Hutto, W.P. Parks, L.L. Rosenblum, K.J. Kunstman, M.R. Furtado, and J.L. Munoz. 1992. Selective transmission of human immunodeficiency virus type-1 variants from mothers to infants. *Science*. 255:1134–1137.
- Zhu, T., H. Mo, N. Wang, D.S. Nam, Y. Cao, R.A. Koup, and D.D. Ho. 1993. Genotypic and phenotypic characterization of HIV-1 patients with primary infection. *Science*. 261:1179–1181.
- Collins, K.B., B.K. Patterson, G.J. Naus, D.V. Landers, and P. Gupta. 2000. Development of an in vitro organ culture model to study transmission of HIV-1 in the female genital tract. *Nat. Med.* 6:475–479.
- Gordon, S.N., R.M. Dunham, J.C. Engram, J. Estes, Z. Wang, N.R. Klatt, M. Paiardini, I.V. Pandrea, C. Apetrei, D.L. Sodora, et al. 2008. Short-lived infected cells support virus replication in sooty mangabeys naturally infected with simian immunodeficiency virus: implications for AIDS pathogenesis. *J. Virol.* 82:3725–3735.
- Hladik, F., P. Sakchalathorn, L. Ballweber, G. Lentz, M. Fialkow, D. Eschenbach, and M.J. McElrath. 2007. Initial events in establishing vaginal entry and infection by human immunodeficiency virus type-1. *Immunity*. 26:257–270.

17. Hu, Q., I. Frank, V. Williams, J.J. Santos, P. Watts, G.E. Griffin, J.P. Moore, M. Pope, and R.J. Shattock. 2004. Blockade of attachment and fusion receptors inhibits HIV-1 infection of human cervical tissue. *J. Exp. Med.* 199:1065–1075.
18. Letvin, N.L., J.R. Mascola, Y. Sun, D.A. Gorgone, A.P. Buzby, L. Xu, Z.Y. Yang, B. Chakrabarti, S.S. Rao, J.E. Schmitz, et al. 2006. Preserved CD4<sup>+</sup> central memory T cells and survival in vaccinated SIV-challenged monkeys. *Science*. 312:1530–1533.
19. Miller, C.J., Q. Li, K. Abel, E.Y. Kim, Z.M. Ma, S. Wietgrefe, L. La Franco-Scheuch, L. Compton, L. Duan, M.D. Shore, et al. 2005. Propagation and dissemination of infection after vaginal transmission of simian immunodeficiency virus. *J. Virol.* 79:9217–9227.
20. Veazey, R.S., R.J. Shattock, M. Pope, J.C. Kirijan, J. Jones, Q. Hu, T. Ketas, P.A. Marx, P.J. Klasse, D.R. Burton, and J.P. Moore. 2003. Prevention of virus transmission to macaque monkeys by a vaginally applied monoclonal antibody to HIV-1 gp120. *Nat. Med.* 9:343–346.
21. McDermott, A.B., J. Mitchen, S. Piaskowski, I. De Souza, L.J. Yant, J. Stephany, J. Furlott, and D.I. Watkins. 2004. Repeated low-dose mucosal simian immunodeficiency virus SIVmac239 challenge results in the same viral and immunological kinetics as high-dose challenge: a model for the evaluation of vaccine efficacy in nonhuman primates. *J. Virol.* 78:3140–3144.
22. Otten, R.A., D.R. Adams, C.N. Kim, E. Jackson, J.K. Pullium, K. Lee, L.A. Grohskopf, M. Monsour, S. Butera, and T.M. Folks. 2005. Multiple vaginal exposures to low doses of R5 simian-human immunodeficiency virus: strategy to study HIV preclinical interventions in nonhuman primates. *J. Infect. Dis.* 191:164–173.
23. Regoes, R.R., I.M. Longini, M.B. Feinberg, and S.I. Staprans. 2005. Preclinical assessment of HIV vaccines and microbicides by repeated low-dose virus challenges. *PLoS Med.* 2:e249.
24. Subbarao, S., R.A. Otten, A. Ramos, C. Kim, E. Jackson, M. Monsour, D.R. Adams, S. Bashirian, J. Johnson, V. Soriano, et al. 2006. Chemoprophylaxis with tenofovir disoproxil fumarate provided partial protection against infection with simian human immunodeficiency virus in macaques given multiple virus challenges. *J. Infect. Dis.* 194:904–911.
25. Fiebig, E.W., D.J. Wright, B.D. Rawal, P.E. Garrett, R.T. Schumacher, L. Peddada, C. Heldebant, R. Smith, A. Conrad, S.H. Kleinman, and M.P. Busch. 2003. Dynamics of HIV viremia and antibody seroconversion in plasma donors: implications for diagnosis and staging of primary HIV infection. *AIDS*. 17:1871–1879.
26. Greenier, J.L., C.J. Miller, D. Lu, P.J. Dailey, F.X. Lu, K.J. Kunstman, S.M. Wolinsky, and M.L. Marthas. 2001. Route of simian immunodeficiency virus inoculation determines the complexity but not the identity of viral variant populations that infect rhesus macaques. *J. Virol.* 75:3753–3765.
27. Nowak, M.A., A.L. Lloyd, G.M. Vasquez, T.A. Wiltout, L.M. Wahl, N. Bischofberger, J. Williams, A. Kinter, A.S. Fauci, V.M. Hirsch, and J.D. Lifson. 1997. Viral dynamics of primary viremia and antiretroviral therapy in simian immunodeficiency virus infection. *J. Virol.* 71:7518–7525.
28. Anderson, J., B.F. Keele, J.F. Salazar-Gonzalez, L.-H. Ping, L. Arney, C. Williamson, G.M. Shaw, B.H. Hahn, M.S. Cohen, and R. Swanstrom. 2009. Determining the genetic linkage of HIV-1 subtype B and C transmission pairs: analyses of viral env sequences from donor and recipient. *16th Conference on Retroviruses and Opportunistic Infections*. Montreal, Canada. Abs. 490.
29. Li, H., B.F. Keele, J.M. Decker, E.E. Giorgi, S. Wang, G.H. Learn, J.F. Salazar-Gonzalez, M.G. Salazar, K. Bar, T. Grayson, et al. 2009. Investigation by single genome amplification of HIV-1 transmission and envelope diversity among men who have sex with men. *16th Conference on Retroviruses and Opportunistic Infections*. Montreal, Canada. Abs. 491.
30. Salazar-Gonzalez, J., M.G. Salazar, B.F. Keele, G.H. Learn, E.E. Giorgi, H. Li, J.M. Decker, S. Wang, J. Baalwa, M.H. Kraus, et al. 2009. Genetic identity, biological phenotype and evolutionary pathways of transmitted/founder viruses in acute and early HIV-1 infection. *J. Exp. Med.* In press.
31. Abrahams, M.-R., J.A. Anderson, E.E. Giorgi, C. Seoghe, K. Mlisana, L.-H. Ping, G.S. Athreya, F.K. Treurnicht, B.F. Keele, N. Wood, et al. 2009. Quantitating the multiplicity of infection with HIV-1 subtype C reveals a non-Poisson distribution of transmitted variants. *J. Virol.* 83:3556–3567.
32. Baalwa, J., S. Wang, B.F. Keele, M.G. Salazar, J.M. Decker, P. Kaleebu, J. Gilmour, E. Cormier, B.H. Hahn, and G.M. Shaw. 2009. Ugandan HIV-1 subtype A, D and AD recombinant transmitted/founder viruses: molecular pathways of evolution and immune escape. *16th Conference on Retroviruses and Opportunistic Infections*. Montreal, Canada. Abs. 488.
33. Haaland, R.E., P.A. Hawkins, J. Salazar-Gonzalez, A. Johnson, A. Tichacek, E. Karita, O. Manigart, J. Mulenga, B.F. Keele, G.M. Shaw, et al. 2009. Inflammatory genital infections mitigate a severe genetic bottleneck in heterosexual transmission of subtype A and C HIV-1. *PLoS Pathog.* 5:e1000274.
34. Kearney, M., F. Maldarelli, W. Shao, J.B. Margolick, E.S. Daar, J.W. Mellors, V. Rao, J.M. Coffin, and S. Palmer. 2009. HIV-1 population genetics and adaptation in newly infected individuals. *J. Virol.* 83:2715–2727.
35. Salazar-Gonzalez, J.F., E. Bailes, K.T. Pham, M.G. Salazar, M.B. Guffey, B.F. Keele, C.A. Derdeyn, P. Farmer, E. Hunter, S. Allen, et al. 2008. Deciphering human immunodeficiency virus type 1 transmission and early envelope diversification by single-genome amplification and sequencing. *J. Virol.* 82:3952–3970.
36. Kirchherr, J.L., X. Lu, W. Kasongo, V. Chalwe, L. Mwananyanda, R.M. Musonda, S.M. Xia, R.M. Searce, H.X. Liao, D.C. Montefiori, et al. 2007. High throughput functional analysis of HIV-1 env genes without cloning. *J. Virol. Methods*. 143:104–111.
37. Palmer, S., M. Kearney, F. Maldarelli, E.K. Halvas, C.J. Bixby, H. Bazmi, D. Rock, J. Falloon, R.T. Davey Jr., R.L. Dewar, et al. 2005. Multiple, linked human immunodeficiency virus type 1 drug resistance mutations in treatment-experienced patients are missed by standard genotype analysis. *J. Clin. Microbiol.* 43:406–413.
38. Shriner, D., A.G. Rodrigo, D.C. Nickle, and J.I. Mullins. 2004. Pervasive genomic recombination of HIV-1 in vivo. *Genetics*. 167:1573–1583.
39. Simmonds, P., P. Balfe, C.A. Ludlam, J.O. Bishop, and A.J. Brown. 1990. Analysis of sequence diversity in hypervariable regions of the external glycoprotein of human immunodeficiency virus type 1. *J. Virol.* 64:5840–5850.
40. Liu, S.L., A.G. Rodrigo, R. Shankarappa, G.H. Learn, L. Hsu, O. Davidov, L.P. Zhao, and J.I. Mullins. 1996. HIV quasispecies and resampling. *Science*. 273:415–416.
41. Letvin, N.L., S.S. Rao, V. Dang, A.P. Buzby, B. Koriath-Schmitz, D. Dombagoda, J.G. Parvani, R.H. Clarke, L. Bar, K.R. Carlson, et al. 2007. No evidence for consistent virus-specific immunity in simian immunodeficiency virus-exposed, uninfected rhesus monkeys. *J. Virol.* 81:12368–12374.
42. Shankarappa, R., J.B. Margolick, S.J. Gange, A.G. Rodrigo, D. Upchurch, H. Farzadegan, P. Gupta, C.R. Rinaldo, G.H. Learn, X. He, et al. 1999. Consistent viral evolutionary changes associated with the progression of human immunodeficiency virus type 1 infection. *J. Virol.* 73:10489–10502.
43. Loffredo, J.T., L.E. Valentine, and D.I. Watkins. 2006/2007. Beyond Mamu-A\*01+ Indian rhesus macaques: continued discovery of new MHC class I molecules that bind epitopes from simian AIDS viruses. *In HIV Molecular Immunology*. B.T.M. Korber, C. Brander, B.F. Haynes, R. Koup, J.P. Moore, B.D. Walker, and D.I. Watkins, editors. Los Alamos National Laboratory, Theoretical Biology and Biophysics, Los Alamos, New Mexico. p. 29–51.
44. O'Connor, D.H., T.M. Allen, T.U. Vogel, P. Jing, I.P. DeSouza, E. Dadds, E.J. Dunphy, C. Melsaether, B. Mothe, H. Yamamoto, et al. 2002. Acute phase cytotoxic T lymphocyte escape is a hallmark of simian immunodeficiency virus infection. *Nat. Med.* 8:493–499.
45. Reynolds, M.R., E. Rakasz, P.J. Skinner, C. White, K. Abel, Z.M. Ma, L. Compton, G. Napoe, N. Wilson, C.J. Miller, et al. 2005. CD8<sup>+</sup> T-lymphocyte response to major immunodominant epitopes after vaginal exposure to simian immunodeficiency virus: too late and too little. *J. Virol.* 79:9228–9235.
46. Drummond, A.J., S.Y. Ho, M.J. Phillips, and A. Rambaut. 2006. Relaxed phylogenetics and dating with confidence. *PLoS Biol.* 4:e88.

47. Drummond, A.J., A. Rambaut, B. Shapiro, and O.G. Pybus. 2005. Bayesian coalescent inference of past population dynamics from molecular sequences. *Mol. Biol. Evol.* 22:1185–1192.
48. Brenchley, J.M., T.W. Schacker, L.E. Ruff, D.A. Price, J.H. Taylor, G.J. Beilman, P.L. Nguyen, A. Khoruts, M. Larson, A.T. Haase, and D.C. Douek. 2004. CD4<sup>+</sup> T cell depletion during all stages of HIV disease occurs predominantly in the gastrointestinal tract. *J. Exp. Med.* 200:749–759.
49. Li, Q., L. Duan, J.D. Estes, Z.M. Ma, T. Rourke, Y. Wang, C. Reilly, J. Carls, C.J. Miller, and A.T. Haase. 2005. Peak SIV replication in resting memory CD4<sup>+</sup> T cells depletes gut lamina propria CD4<sup>+</sup> T cells. *Nature*. 434:1148–1152.
50. Mehandru, S., M.A. Poles, K. Tenner-Racz, A. Horowitz, A. Hurley, C. Hogan, D. Boden, P. Racz, and M. Markowitz. 2004. Primary HIV-1 infection is associated with preferential depletion of CD4<sup>+</sup> T lymphocytes from effector sites in the gastrointestinal tract. *J. Exp. Med.* 200:761–770.
51. Veazey, R.S., M. DeMaria, L.V. Chalifoux, D.E. Shvetz, D.R. Pauley, H.L. Knight, M. Rosenzweig, R.P. Johnson, R.C. Desrosiers, and A.A. Lackner. 1998. Gastrointestinal tract as a major site of CD4<sup>+</sup> T cell depletion and viral replication in SIV infection. *Science*. 280:427–431.
52. Veazey, R.S., and A.A. Lackner. 2004. Getting to the guts of HIV pathogenesis. *J. Exp. Med.* 200:697–700.
53. Ma, Z.M., K. Abel, T. Rourke, Y. Wang, and C.J. Miller. 2004. A period of transient viremia and occult infection precedes persistent viremia and antiviral immune responses during multiple low-dose intravaginal simian immunodeficiency virus inoculations. *J. Virol.* 78:14048–14052.
54. McChesney, M.B., J.R. Collins, D. Lu, X. Lu, J. Torten, R.L. Ashley, M.W. Cloyd, and C.J. Miller. 1998. Occult systemic infection and persistent simian immunodeficiency virus (SIV)-specific CD4(+)–T-cell proliferative responses in rhesus macaques that were transiently viremic after intravaginal inoculation of SIV. *J. Virol.* 72:10029–10035.
55. Miller, C.J. 1994. Mucosal transmission of simian immunodeficiency virus. *Curr. Top. Microbiol. Immunol.* 188:107–122.
56. Miller, C.J., N.J. Alexander, S. Sutjipto, A.A. Lackner, A. Gettie, A.G. Hendrickx, L.J. Lowenstine, M. Jennings, and P.A. Marx. 1989. Genital mucosal transmission of simian immunodeficiency virus: animal model for heterosexual transmission of human immunodeficiency virus. *J. Virol.* 63:4277–4284.
57. Busch, M.P., E.A. Operskalski, J.W. Mosley, T.H. Lee, D. Henrard, S. Herman, D.H. Sachs, M. Harris, W. Huang, and D.O. Stram. 1996. Factors influencing human immunodeficiency virus type 1 transmission by blood transfusion. Transfusion Safety Study Group. *J. Infect. Dis.* 174:26–33.
58. Powers, K.A., C. Poole, A.E. Pettifor, and M.S. Cohen. 2008. Rethinking the heterosexual infectivity of HIV-1: a systematic review and meta-analysis. *Lancet Infect. Dis.* 8:553–563.
59. Stafford, M.A., L. Corey, Y. Cao, E.S. Daar, D.D. Ho, and A.S. Perelson. 2000. Modeling plasma virus concentration during primary HIV infection. *J. Theor. Biol.* 203:285–301.
60. Wilson, N.A., B.F. Keele, J.S. Reed, S.M. Piaskowski, C.E. Mac Nair, A. Bett, X. Liang, F. Wang, E. Thoryk, G. Heidecker, et al. 2009. Vaccine-induced cellular responses control SIV replication after heterologous challenge. *J. Virol.* In press.
61. Simon, V., V. Zennou, D. Murray, Y. Huang, D.D. Ho, and P.D. Bieniasz. 2005. Natural variation in Vif: differential impact on APOBEC3G/3F and a potential role in HIV-1 diversification. *PLoS Pathog.* 1:e6.
62. Pilcher, C.D., G. Joaki, I.F. Hoffman, F.E. Martinson, C. Mapanje, P.W. Stewart, K.A. Powers, S. Galvin, D. Chilongozi, S. Gama, et al. 2007. Amplified transmission of HIV-1: comparison of HIV-1 concentrations in semen and blood during acute and chronic infection. *AIDS*. 21:1723–1730.
63. Quinn, T.C., M.J. Wawer, N. Sewankambo, D. Serwadda, C. Li, F. Wabwire-Mangen, M.O. Meehan, T. Lutalo, and R.H. Gray. 2000. Viral load and heterosexual transmission of human immunodeficiency virus type 1. Rakai Project Study Group. *N. Engl. J. Med.* 342:921–929.
64. Wawer, M.J., R.H. Gray, N.K. Sewankambo, D. Serwadda, X. Li, O. Laeyendecker, N. Kiwanuka, G. Kigozi, M. Kiddugavu, T. Lutalo, et al. 2005. Rates of HIV-1 transmission per coital act, by stage of HIV-1 infection, in Rakai, Uganda. *J. Infect. Dis.* 191:1403–1409.
65. Thompson, J.D., D.G. Higgins, and T.J. Gibson. 1994. CLUSTAL W: improving the sensitivity of progressive multiple sequence alignment through sequence weighting, position-specific gap penalties and weight matrix choice. *Nucleic Acids Res.* 22:4673–4680.
66. Kosakovsky Pond, S.L., D. Posada, M.B. Gravenor, C.H. Woelk, and S.D. Frost. 2006. Automated phylogenetic detection of recombination using a genetic algorithm. *Mol. Biol. Evol.* 23:1891–1901.
67. Maydt, J., and T. Lengauer. 2006. Recco: recombination analysis using cost optimization. *Bioinformatics*. 22:1064–1071.